that *ABCA12* expression in differentiating cultured human keratinocytes is critically dependent on a palindromic motif that resides in the region of −2084 to −2078 from the transcription start site (TSS).

Results

Identification of the critical region of −2200 to −1934 in the upstream promoter of the *ABCA12* gene. To locate the essential elements in the upstream region of ABCA12, we first cloned a −2980/+190 fragment (the base position +1 is the TSS of *ABCA12*, chr2: 216,003,151) and performed a dual luciferase reporter assay to assess its promoter activity with respect to keratinocyte differentiation status. We utilized cultured normal human epidermal keratinocytes (NHEK). It is well established that increased cellular calcium level is a key signal to promote the differentiation of keratinocytes in culture as well as in normal skin[10,11]. Accordingly, NHEKs differentiate under the high-calcium condition, and ABCA12 expression increases in differentiated keratinocytes[1,2]. As expected, the −2980/+190 fragment showed 3.2 times as much activity when NHEKs were cultured under the high-calcium condition (1.2 mM) compared to the low-calcium condition (0.06 mM) (Fig. 1, Supplementary Fig. S1). We performed an *in silico* search of the ENCODE dataset using the UCSC genomic browser[12] throughout this region and found increased ChIP-seq signals and peaks of H3K4me3 and H3K27ac, and increased DNAseI-seq peaks in NHEK (Fig. 2). These results were considered to support the bona fide promoter function of this genetic region. Additionally, an *in silico* analysis using JASPAR CORE database (http://jaspar.genereg.net/)[13] found 398 putative transcription factor binding sites within this region.

We then aimed to narrow down the region that contains the essential promoter elements experimentally. For this purpose, increasing lengths of the upstream region of the *ABCA12* gene were cloned and their promoter activities were assessed by a dual luciferase reporter assay (Fig. 1, Supplementary Fig. S1). Under the high-calcium condition, the highest promoter activity was detected with the −2980/+190 fragment, whereas −1994/+190 and −1039/+190 fragments showed drastically decreased promoter activity (−12.2 fold, $P < 0.01$ and −6.41 fold, $P < 0.01$ compared to the −2980/+190 fragment, respectively). These results suggest that one or more critical promoter elements may reside within the region from −2980 to −1994 of the *ABCA12* promoter.

To further narrow the region containing the putative element(s), promoter activity was analyzed for five serially truncated fragments consisting of the −2980/+190 to −1934/+190 *ABCA12* upstream region (Fig. 3a, Supplementary Fig. S2). Under the high-calcium condition, the 2700/+190 fragment showed roughly comparable promoter activity to the −2980/+190 fragment (−1.43 fold compared to the −2980/+190 fragment, not significant), whereas the −1994/+190 fragment showed markedly reduced promoter activity (−16.1 fold compared to the −2980/+190 fragment, $P < 0.01$). Promoter activities of the −2400/+190 to −2200/+190 fragments were decreased compared with that of the −2980/+190 fragment (−2.28 fold, $P < 0.01$ and 35.3%, $P < 0.01$, respectively). Therefore, we considered that the region from −2700 to −1994 is critical for the promoter activity of the ABCA12 upstream region in NHEK.

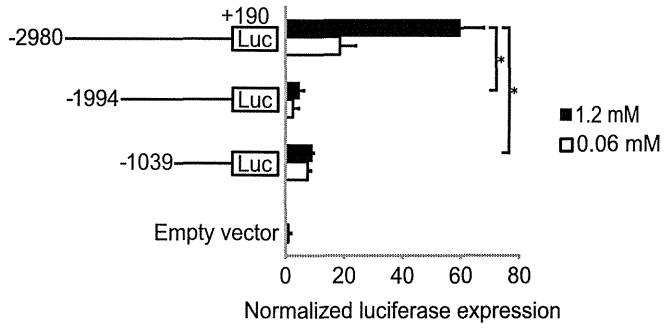

Figure 1 | Position −2980 to position −1994 of the *ABCA12* gene has promoter activity. Dual luciferase assay was performed using *firefly* luciferase reporter vectors that contain −2980/+190, −1994/+190 or −1039/+190 fragments of the *ABCA12* gene. The culture medium contained either 0.06 mM or 1.2 mM calcium. The promoter activities are normalized using the empty vector as a standard. The bars represent the standard deviation (n = 3). *$P < 0.01$ compared with the −2980/+190 fragment.

To identify the most critical region between −2700 and −1994, four short overlapping fragments spanning the region were cloned and their promoter activities were assessed (Fig. 3b, Supplementary Fig. S2b). The −2200/−1934 fragment showed the highest promoter activity, suggesting that this region may contain the critical element(s) (Fig. 3b, Supplementary Fig. S2).

Interestingly, the promoter activity of this fragment was not dependent on the increased calcium concentration, suggesting that an unknown element outside the −2200/−1934 region may exist to suppress the activity under low-calcium conditions. The neighboring −2400/−2106 fragment also showed some promoter activity, although not as much as the −2200/−1934 fragment.

A palindromic motif in the −2084 to −2078 region is essential for the promoter activity. To pinpoint the critical bases that could be used for the genetic diagnostic screening of congenital ichthyosis patients, we searched for consensus sequences for transcription factor binding elements within the region from −2200 to −1934. An *in silico* analysis using the JASPAR CORE database found a predicted specificity protein 1 (Sp1) binding motif (−2133 to −2144, reverse strand, chr2:216,005,284–216,005,295) and a palindromic motif that matches an AP1 binding sequence (tgagtca, −2084 to −2078, chr2:216,005,235–216,005,228) within the −2200/−1934 fragment (Fig. 2, Supplementary Fig. S3).

The AP1 elements may be able to tether AP1 transcription factors to the promoter region of the genome and regulate downstream gene expression. In keratinocytes, AP1 regulates the expression of various genes, such as involucrin and transglutaminase 1[14]; these AP1-regulated genes are involved in keratinocyte differentiation and are mostly expressed in the late stage of terminal differentiation[15]. When these motifs were mapped in the ENCODE dataset annotations using the UCSC genome browser, the palindromic −2084/−2078 motif was found to reside within the increased ChIP-seq signals of H3K4me3 and H3K27ac, and within the DNAseI-seq peak in NHEK (Fig. 2).

These considerations lead us to hypothesize that the −2084/−2078 motif may regulate the expression of ABCA12. Therefore, we introduced one to three nucleotide deletion mutations into the wild-type sequence (tgagtca): mutant Δ1 (tga-tca), mutant Δ2 (tga--ca) and mutant Δ3 (tg---ca). We investigated the effect of the mutations on the promoter activity of the −2980/+190 fragment (Fig. 4, Supplementary Fig. S4). All three mutants showed strikingly reduced promoter activity compared to the wild type (−6.10 fold, $P < 0.01$, −9.71 fold, $P < 0.01$ and −11.7 fold, $P < 0.01$ for Δ1, Δ2 and Δ3, respectively) (Fig. 4, Supplementary Fig. S4). No significant differences in promoter activity were found between the three mutants.

Discussion

The present results clearly demonstrate that disruption of the −2084/−2078 motif alone can critically decrease the promoter activity of the entire 3 kb upstream sequence of *ABCA12*. In addition, the 267 bp fragment containing this motif (−2200/−1934) is sufficient to establish potent promoter activity. This experiment using short genomic fragments may have the shortcoming that the assays are done without the context of their original core promoters or other minimal promoters, and the interpretation of the results may be

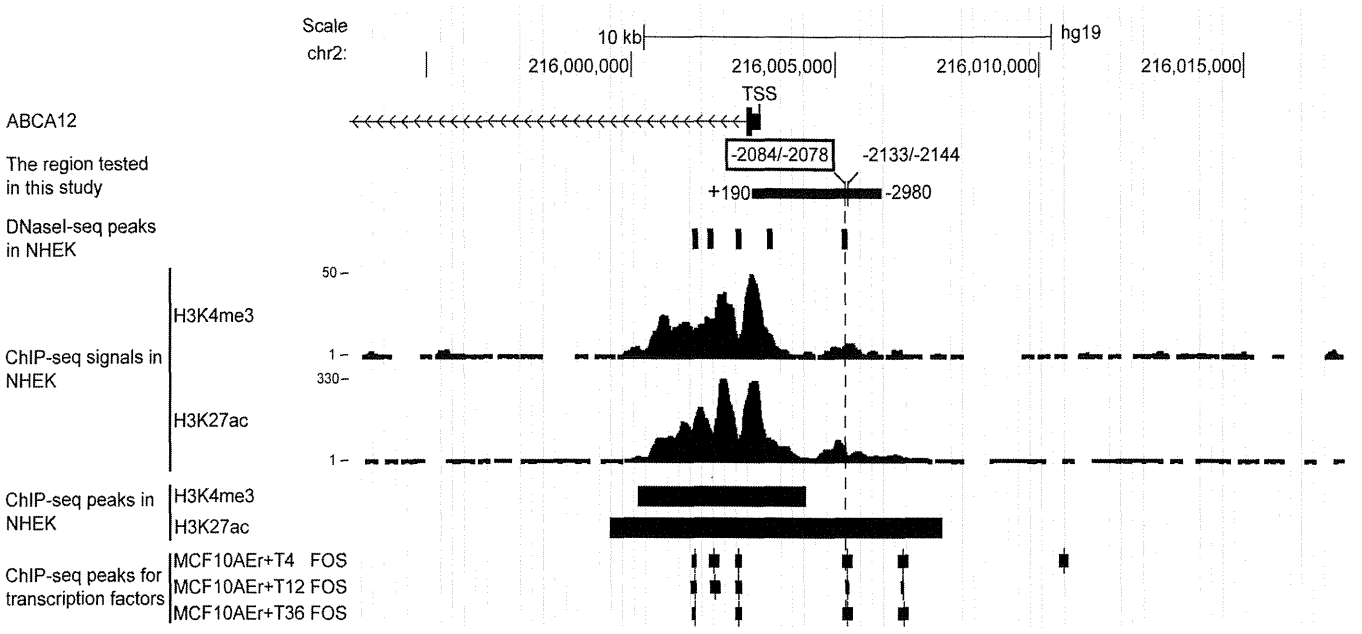

Figure 2 | Annotation of the ABCA12 upstream gene using the ENCODE dataset. The ABCA12 upstream genomic region (chr2:215,993,140–216,017,439:GRCh37/hg19) is illustrated using the UCSC genome browser. ChIP-seq signals and peaks of H3K4me3 and H3K27ac, and DNaseI-seq peaks in NHEK were extracted from the ENCODE dataset and annotated. The read density of ChIP-seq signals is indicated in the Y-axis. ChIP-seq peaks of c-Fos/c-Jun in 91 human cell types from the ENCODE dataset are also shown. c-Fos peaks for MCF10A-Er-Src cells stimulated with tamoxifen for 4 hr (MCF10AEr + T4 FOS), 12 hr (MCF10AEr + T12 FOS), or 36 hr (MCF10AEr + T36 FOS) were found in the database search. The −2084/−2078 palindromic motif is boxed, and its genetic location is highlighted with a dotted line. The predicted −2133/−2144 Sp1 binding element is also indicated.

limited to the demonstration of a possible capability of each fragment to recruit transcription factors. The following mutagenesis experiment thus confirmed the essential role of the −2084/−2078 motif in its native genomic context. In support of these results, the ENCODE dataset search showed increased ChIP-seq signals for H3K4me3 and H3K27ac, which mark active promoters, and a DNaseI-seq peak that demonstrates the open chromatin state in NHEK. Interestingly, in MCF10A-Er-Src cells stimulated with tamoxifen, the ChIP-seq tag containing this motif is associated with a peak for c-Fos, a component of AP1 (Fig. 2), showing that the motif may indeed recruit these transcription factors in certain cells, although it is not yet proven whether c-Fos binds the −2084/−2078 motif in NHEK. In agreement with the experimentally proven significance of this motif, a database search shows a high conservation of the −2084/−2078 sequence among multiple eutherian species (Supplementary Fig. S5). We searched for previously reported SNPs in the HAPMAP database[16] in this genetic region, but we found no SNP in the −2084/−2078 sequence in populations with European or Asian ancestry.

Apart from the −2084/−2078 motif, the −2200/−1934 fragment harbors a predicted −2133/−2144 Sp1 binding element. It is reported that AP1 and Sp1 cooperatively regulate the expression of target genes in keratinocytes, such as *LOR*, which encodes loricrin[17]. Therefore, it may be assumed that the expression of ABCA12 is also regulated by the putative −2133/−2144 element. Nevertheless, in the actual context of the entire promoter sequences, the predicted element may play rather an adjunctive role in *ABCA12* expression, because the disruption of the −2084/−2078 motif alone is sufficient to reduce the promoter activity of the −2980/+190 fragment to one-tenth of its original activity.

In the present study, we are aware of the limitation of depending solely on luciferase assays performed on NHEK, as they do not provide direct evidence for the function of the −2084/−2078 motif in its true genomic context. However, the existing ChIP-seq and DNaseI-seq results obtained from NHEK are in accordance with the proposed function of this motif as the essential promoter element and can reinforce the conclusions obtained from our experiments.

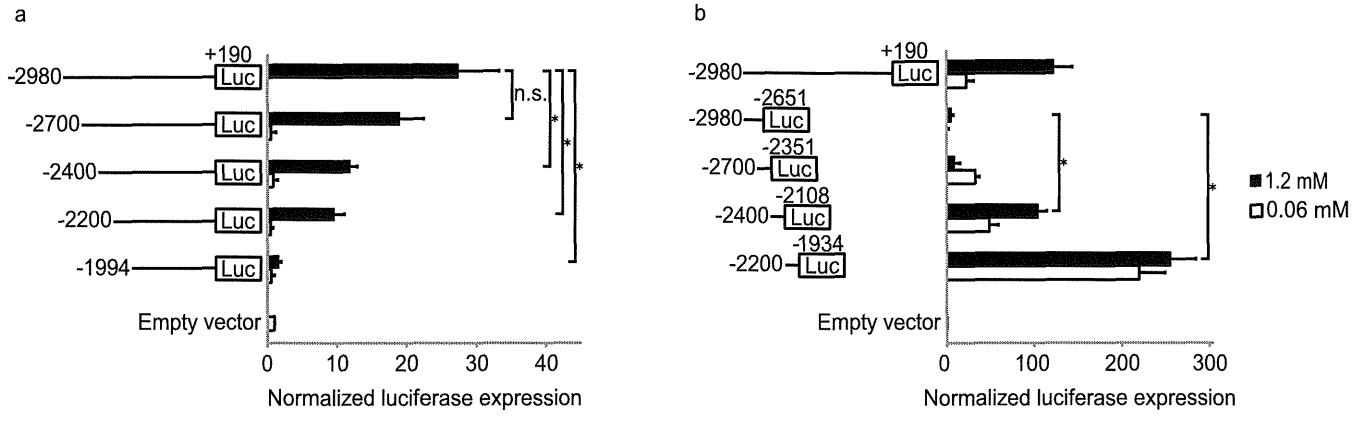

Figure 3 | Position −2200 to position −1934 of the *ABCA12* gene exhibits potent promoter activity. Promoter activities of −2980/+190, −2700/+190, −2400/+190, −2200/+190, or −1994/+190 fragments (a), and −2980/−2651, −2700/−2351, −2400/−2108, or −2200/−1934 fragments (b) were assayed. *$P < 0.01$ compared with the −2980/+190 fragment (a) or the −2980/−2651 fragment (b).

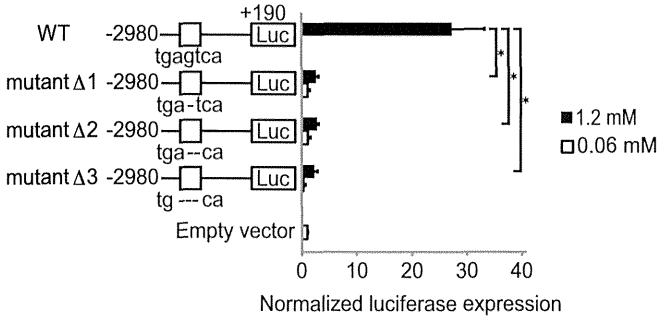

Figure 4 | Mutants of the −2084/−2078 motif in *ABCA12* show striking reduction of promoter activity. Three different mutants of the −2084/−2078 motif were generated using the −2980/+190 fragment as a template, and the promoter activity of each fragment was assessed. The mutants lacked 1–3 bases from the wild-type sequence (tgagtca): mutant Δ1 (tga-tca), mutant Δ2 (tga--ca) and mutant Δ3 (tg---ca). The promoter activities of the mutants were compared to that of the wild type. *$P < 0.01$ compared with the wild type.

From these considerations, we propose that future routine genetic screening for the diagnosis of congenital ichthyosis patients include the sequencing of the −2084/−2078 upstream region of *ABCA12*, especially if *ABCA12* mutation is detected in one of the patient's allele. We sequenced the −2200/−1934 *ABCA12* upstream region of five autosomal recessive congenital ichthyosis patients. These patients showed decreased *ABCA12* mRNA expression; however, known pathogenic mutations within *ABCA12* exons or exon-intron boundaries were found in only one allele of each patient. Although no mutations were detected in this limited number of patients (data not shown), the screening of future patients could benefit from sequencing of the genetic region.

This report describes the −2084/−2078 palindromic motif upstream of the *ABCA12* gene as a promoter element. However, it may be more precisely termed an enhancer element, because it is farther upstream of the core promoter that neighbors the TSS of *ABCA12*. Nevertheless, there is no widely accepted standard for differentiating between a promoter element and an enhancer element. Considering the comparative proximity of the motif (2.1 kb from TSS), we propose that it may be reasonably termed a promoter element.

It is of interest that the −2200/−1934 fragment exhibited potent promoter activity in the low-calcium condition as well as in the high-calcium condition. Since the −2980/+190 fragment shows a marked calcium-dependent upregulation of its promoter activity, it may be suggested that an unknown suppressor element(s) exists outside the −2200/−1934 region and functions specifically under low-calcium conditions. However, suppressor elements would not warrant the genetic sequencing of autosomal recessive congenital ichthyosis patients and is beyond the scope of the present study.

Methods

Ethics statement. This study was approved by the Medical Ethics Committee of Nagoya University (#1088), and performed according to the Declaration of Helsinki Principles. The participants gave written informed consent. Written informed consent was obtained from the guardians on behalf of the children enrolled. We recorded participant consent in paper. The ethic committee approved the consent procedure.

Construction of plasmids. To determine the promoter region of the *ABCA12* gene, a series of luciferase reporter plasmids were generated. PCR fragments containing upstream regions of the human *ABCA12* gene (NCBI Reference Sequence: NG_007074.1, http://www.ncbi.nlm.nih.gov/) of increasing lengths were amplified using specific primers (Table 1). The fragments were subcloned using the In-Fusion HD Cloning Kit (Clontech) into a pGL4.10 basic vector (Promega) that contains the *firefly* luciferase gene but does not contain any eukaryotic regulatory elements. All of the produced vectors were verified.

Cell culture and transfection. Normal human epidermal keratinocytes (NHEKs) were cultured in EpiLife (Gibco) supplemented with human keratinocyte growth supplement (HKGS; Gibco) at 37°C under 5% CO_2. For transfection of the plasmid vectors, the NHEKs were seeded on 24-well plates (1.0×10^5 cells/ml). At 50–70% confluence, the cells were washed once with PBS. Transfection was then performed by adding 0.5 μg of *firefly* luciferase reporter vector and 0.05 μg of pGL4.74 [*hRluc*/TK] *renilla* luciferase reporter vector (Promega) mixed with TransIT-Keratinocyte Transfection Reagent (Mirus) in EpiLife, and incubating for 20 min at 25°C. The transfected NHEKs were incubated for 6 h at 37°C with the mixture, and then the medium was changed to EpiLife/HKGS supplemented with either 0.06 mM or 1.2 mM calcium.

Dual-luciferase reporter assay. The NHEKs were incubated in either low (0.06 mM) or high (1.2 mM) calcium condition for 48 h after transfection. Then, the promoter activity was measured by Dual-Luciferase Reporter Assay System (Promega) using the GloMax-Multi Detection System (Promega) according to manufacturer's protocol. All experiments were performed in triplicate. The promoter activity was calculated as the ratio of *firefly* luciferase reporter expression to Renilla luciferase reporter expression that is driven by the *Herpes simplex* virus thymidine kinase promoter contained in the pGL4.74[*hRluc*/TK] vector.

In silico analysis of transcription factors. We performed *in silico* analysis to reveal potential transcription binding elements in the upstream region of the *ABCA12* gene using the JASPAR CORE database (http://jaspar.genereg.net/)[13]. The sequence was scanned with JASPER CORE vertebrata matrix models with a relative profile score threshold of 90%.

ENCODE and HAPMAP data set search and comparative multiple alignments. A series of database searches was performed using the UCSC Genome Browser database; ENCODE dataset for ChIP-seq signals and peaks of H3K4me3 and H3K27ac in NHEK, DNAseI-seq peaks in NHEKs, transcription factor ChIP-seq peaks of c-Fos/c-Jun in 91 human cell types, and SNPs from HAPMAP datasets[12,16,18]. All genomic annotations are mapped on genome assembly GRCh37/hg19. The multiple alignments of the conserved AP1 element among 55 vertebrae species were also obtained and the alignment and consensus logo was generated with CLC Main Workbench software (CLC Bio).

Table 1 | PCR Primers for cloning of the promoter region of *ABCA12*

Fragment	Forward primer	Reverse primer
−2980/+190	gctcgctagcctcgaacttgttgcacatttccacc	cgccgaggccagatctcttcttttctccactccac
−1994/+190	gctcgctagcctcgagtattctagcagatggcagg	cgccgaggccagatctcttcttttctccactccac
−1039/+190	gctcgctagcctcgaactagccttggctccagtag	cgccgaggccagatctcttcttttctccactccac
−2980/−2651	gctcgctagcctcgaacttgttgcacatttccacc	cgccgaggccagatctctcagcactggttg
−2700/−2351	gctcgctagcctcgacaaacaaacaaagtt	cgccgaggccagatcctaagagctggtctg
−2400/−2108	gctcgctagcctcgaggtccctaactctcc	cgccgaggccagatcttttccagcacttcc
−2200/−1934	gctcgctagcctcgactatctgtgcgaaca	cgccgaggccagatctgccagcttcatcag
−2980/+190	gctcgctagcctcgaacttgttgcacatttccacc	cgccgaggccagatctcttcttttctccactccac
−2700/+190	gctcgctagcctcgacaaacaaacaaagtt	cgccgaggccagatctcttcttttctccactccac
−2400/+190	gctcgctagcctcgaggtccctaactctcc	cgccgaggccagatctcttcttttctccactccac
−2200/+190	gctcgctagcctcgactatctgtgcgaaca	cgccgaggccagatctcttcttttctccactccac
mutant Δ1	acacttgatcagtcatttgagaatgagcacaat	atgactgatcaagtgtaacttcccctctgaagc
mutant Δ2	tacacttgtcagtcatttgagaatgagcacaat	aatgactgacaagtgtaacttcccctctgaagc
mutant Δ3	ttacacttgcagtcatttgagaatgagcacaat	aaatgactgcaagtgtaacttcccctctgaagc

Mutation analysis. To confirm the promoter activity of the −2084/−2078 motif (TGAGTCA), three different mutants were constructed by inverse PCR using the pGL4.10 −2980/+190 reporter as a template (Table 1). The three mutants lacked 1–3 bases from the wild-type sequence (wild-type AP1, tgagtca; mutant Δ1, tga-tca; mutant Δ2, tga--ca; mutant Δ3, tg---ca). Promoter activities of reporter vectors containing the mutants were analyzed and compared with that of the wild type.

Statistics. Statistical analyses were performed with the GraphPad Prism software version 5.04 (GraphPad Software). One-way analysis of variance (ANOVA) with Tukey post hoc test was used to determine statistical significance. A P value of <0.05 was considered significant.

1. Sakai, K. *et al.* Localization of ABCA12 from Golgi apparatus to lamellar granules in human upper epidermal keratinocytes. *Exp Dermatol* **16**, 920–926, doi:10.1111/j.1600-0625.2007.00614.x (2007).
2. Annilo, T. *et al.* Identification and characterization of a novel ABCA subfamily member, ABCA12, located in the lamellar ichthyosis region on 2q34. *Cytogenet Genome Res* **98**, 169–176, doi:69811 (2002).
3. Akiyama, M. *et al.* Mutations in lipid transporter ABCA12 in harlequin ichthyosis and functional recovery by corrective gene transfer. *J Clin Invest* **115**, 1777–1784, doi:10.1172/JCI24834 (2005).
4. Akiyama, M. The roles of ABCA12 in keratinocyte differentiation and lipid barrier formation in the epidermis. *Dermatoendocrinol* **3**, 107–112, doi:10.4161/derm.3.2.15136 (2011).
5. Kelsell, D. P. *et al.* Mutations in ABCA12 underlie the severe congenital skin disease harlequin ichthyosis. *Am J Hum Genet* **76**, 794–803, doi:10.1086/429844 (2005).
6. Lefevre, C. *et al.* Mutations in the transporter ABCA12 are associated with lamellar ichthyosis type 2. *Hum Mol Genet* **12**, 2369–2378, doi:10.1093/hmg/ddg235 (2003).
7. Natsuga, K. *et al.* Novel ABCA12 mutations identified in two cases of non-bullous congenital ichthyosiform erythroderma associated with multiple skin malignant neoplasia. *J Invest Dermatol* **127**, 2669–2673, doi:10.1038/sj.jid.5700885 (2007).
8. Akiyama, M. ABCA12 mutations and autosomal recessive congenital ichthyosis: a review of genotype/phenotype correlations and of pathogenetic concepts. *Hum Mutat* **31**, 1090–1096, doi:10.1002/humu.21326 (2010).
9. Takeichi, T., Sugiura, K., Matsuda, K., Kono, M. & Akiyama, M. Novel ABCA12 splice site deletion mutation and ABCA12 mRNA analysis of pulled hair samples in harlequin ichthyosis. *J Dermatol Sci* **69**, 259–261, doi:10.1016/j.jdermsci.2012.11.004 (2013).
10. Hennings, H. *et al.* Calcium regulation of growth and differentiation of mouse epidermal cells in culture. *Cell* **19**, 245–254 (1980).
11. Menon, G. K., Grayson, S. & Elias, P. M. Ionic calcium reservoirs in mammalian epidermis: ultrastructural localization by ion-capture cytochemistry. *J Invest Dermatol* **84**, 508–512 (1985).
12. Kellis, M. *et al.* Defining functional DNA elements in the human genome. *Proc Natl Acad Sci U S A* **111**, 6131–6138 (2014).
13. Mathelier, A. *et al.* JASPAR 2014: an extensively expanded and updated open-access database of transcription factor binding profiles. *Nucleic acids research* **42**, D142–147, doi:10.1093/nar/gkt997 (2014).
14. Rossi, A., Jang, S. I., Ceci, R., Steinert, P. M. & Markova, N. G. Effect of AP1 transcription factors on the regulation of transcription in normal human epidermal keratinocytes. *J Invest Dermatol* **110**, 34–40, doi:10.1046/j.1523-1747.1998.00071.x (1998).
15. Yamada, K. *et al.* Activation of the human transglutaminase 1 promoter in transgenic mice: terminal differentiation-specific expression of the TGM1-lacZ transgene in keratinized stratified squamous epithelia. *Hum Mol Genet* **6**, 2223–2231 (1997).
16. International HapMap Consortium. A second generation human haplotype map of over 3.1 million SNPs. *Nature* **449**, 851–861 (2007).
17. Jang, S. I. & Steinert, P. M. Loricrin expression in cultured human keratinocytes is controlled by a complex interplay between transcription factors of the Sp1, CREB, AP1, and AP2 families. *J Biol Chem* **277**, 42268–42279, doi:10.1074/jbc.M205593200 (2002).
18. Karolchik, D. *et al.* The UCSC Genome Browser database: 2014 update. *Nucleic Acids Res* **42**, D764–770, doi:10.1093/nar/gkt1168 (2014).

Acknowledgments

This work was supported in part by Grant-in-aid for Scientific Research (A) 23249058 to M.A. from the Ministry of Education, Culture, Sports, Science and Technology of Japan (http://www.mext.go.jp/english/), a grant from the Ministry of Health, Labor and Welfare of Japan (http://www.mhlw.go.jp/stf/seisakunitsuite/bunya/hokabunya/kenkyujigyou/) (Health and Labor Sciences Research Grant: Research on Intractable Diseases; H22-Nanchi-Ippan-177) to M.A, a grant from the Ministry of Health, Labor and Welfare of Japan (http://www.mhlw.go.jp/stf/seisakunitsuite/bunya/hokabunya/kenkyujigyou/) (Health and Labor Sciences Research Grant: Research on Intractable Diseases; H25-Nanchi-Ippan-003) to M.A., and a grant to Y.O from the Japan Intractable Diseases Research Foundation (http://www.nanbyou.jp/). The funders had no role in study design, data collection and analysis, decision to publish, or preparation of the manuscript.

Author contributions

Y.S., T.Y., A.K., D.S., S.H. and M.A. designed the experiments. Y.S., K.S.-S. and T.Y. performed the experiments. Y.S., J.T. and K.S. performed genetic analyses. K.S. and M.A. provided clinical samples. Y.S., Y.O., K. Sakai, T.Y. and M.A. analyzed the data. Y.S., Y.O. and M.A. wrote the paper.

Additional information

Supplementary information accompanies this paper at http://www.nature.com/scientificreports

Competing financial interests: The authors declare no competing financial interests.

How to cite this article: Shimizu, Y. *et al.* A Palindromic Motif in the −2084 to −2078 Upstream Region is Essential for ABCA12 Promoter Function in Cultured Human Keratinocytes. *Sci. Rep.* **4**, 6737; DOI:10.1038/srep06737 (2014).

ELSEVIER

Brain & Development 37 (2015) 418–422

BRAIN & DEVELOPMENT
Official Journal of the Japanese Society of Child Neurology

www.elsevier.com/locate/braindev

Original article

Efficacy and safety of fosphenytoin for acute encephalopathy in children

Mika Nakazawa [a,b,*], Manami Akasaka [c], Takeshi Hasegawa [d], Tomonori Suzuki [e], Taiki Shima [a,f], Jun-ichi Takanashi [g], Atsuko Yamamoto [h], Yuuki Ishidou [i], Kenjiro Kikuchi [j], Shinichi Niijima [b], Toshiaki Shimizu [a], Akihisa Okumura [a,k]

[a] *Department of Pediatrics, Juntendo University Faculty of Medicine, Japan*
[b] *Department of Pediatrics, Juntendo University Nerima Hospital, Japan*
[c] *Department of Pediatrics, Iwate Medical University Faculty of Medicine, Japan*
[d] *Department of Pediatrics, Soka Municipal Hospital, Japan*
[e] *Department of Pediatrics, Kawaguchi Municipal Medical Center, Japan*
[f] *Department of Neuropediatrics, Nagano Children's Hospital, Japan*
[g] *Department of Pediatrics, Kameda Medical Center, Japan*
[h] *Department of Pediatrics, Tsuchiura Kyodo General Hospital, Japan*
[i] *Department of Pediatrics, St. Mary's Hospital, Japan*
[j] *Division of Neurology, Saitama Children's Medical Center, Japan*
[k] *Department of Pediatrics, Aichi Medical University, Japan*

Received 1 May 2014; received in revised form 20 June 2014; accepted 20 June 2014

Abstract

Purpose: To evaluate the efficacy and safety of fosphenytoin (fPHT) for the treatment of seizures in children with acute encephalopathy.

Methods: Using responses from physicians on the Annual Zao Conference on Pediatric Neurology mailing list we chose patients who met the following criteria: clinical diagnosis of acute encephalopathy and use of intravenous fPHT for the treatment of seizures. We divided the patients into two groups: acute encephalopathy with biphasic seizures and late reduced diffusion (AESD) and other encephalopathies. The efficacy of fPHT was considered effective when a cessation of seizures was achieved.

Results: Data of 38 children were obtained (median age, 27 months). Eighteen children were categorized into the AESD group and 20 into the other encephalopathies group. fPHT was administered in 48 clinical events. The median loading dose of fPHT was 22.5 mg/kg and was effective in 34 of 48 (71%) events. The rate of events in which fPHT was effective did not differ according to the presence or absence of prior antiepileptic treatment, subtype of acute encephalopathy, or the type of seizures. One patient experienced apnea and oral dyskinesia as adverse effects of fPHT, whereas arrhythmia, hypotension, obvious reduction of consciousness, local irritation, phlebitis and purple grove syndrome were not observed in any patient.

Conclusion: fPHT is effective and well tolerated among children with acute encephalopathy.

Keywords: Fosphenytoin; Acute encephalopathy; Acute encephalopathy with biphasic seizures and late reduced diffusion; Efficacy; Safety

* Corresponding author. Address: Department of Pediatrics, Juntendo University Faculty of Medicine, 2-1-1 Hongo, Bunkyo-ku, Tokyo 113-8421, Japan. Tel.: +81 3 3813 3111; fax: +81 3 5800 1580.
E-mail address: mknakaza@juntendo.ac.jp (M. Nakazawa).

http://dx.doi.org/10.1016/j.braindev.2014.06.009
0387-7604/

1. Introduction

Seizures are one of the most common neurological symptoms among children with acute encephalopathy and evolve often into status epilepticus. The early cessation of seizures is generally accepted as desirable to improve the outcome in children with encephalopathy. However, seizures in children with acute encephalopathy are often refractory to antiepileptic drugs.

Recently in Japan, treatment for acute encephalopathy with biphasic seizures and late reduced diffusion (AESD), a characteristic subtype of acute encephalopathy in children, has become an important issue. AESD is characterized by prolonged seizure onset or status epilepticus followed by secondary seizures (late seizures) associated with deterioration of consciousness and widespread reduced diffusion in the subcortical white matter on magnetic resonance imaging (MRI) [1]. Late seizures occur usually in clusters and are refractory to antiepileptic drugs. Seizure control is also important in children with other subtypes of acute encephalopathy, such as acute necrotizing encephalopathy (ANE) [2] and acute disseminated encephalomyelitis (ADEM).

Phenytoin (PHT) is a useful antiepileptic drug for the treatment of seizures in children with acute encephalopathy. PHT has a lesser effect on the level of consciousness [3] and we previously reported its efficacy for seizures in children with AESD [4]. However, PHT has been known to occasionally cause local irritation, phlebitis and intravenous fluid incompatibility. Purple glove syndrome is also known as a rare but serious side effect of PHT. Thus, pediatricians and pediatric neurologists in Japan tend to avoid administering PHT. Fosphenytoin (fPHT) is a water-soluble prodrug of PHT with a neutral pH value. The adverse effects of fPHT are less frequent than those of PHT. fPHT was marketed in Japan in 2011 and given to children with several subtypes of acute encephalopathy. At present, the efficacy and safety of fPHT for the treatment of acute encephalopathy in children have not been elucidated. We collected clinical data of children with acute encephalopathy treated with fPHT to determine its efficacy and safety. We also focused on the efficacy of fPHT in Japanese children with AESD, a common and problematic subtype of acute encephalopathy [5].

2. Methods

Using responses from physicians on the Annual Zao Conference on Pediatric Neurology mailing list we chose patients who met the following criteria: clinical diagnosis of acute encephalopathy and use of intravenous fPHT for the treatment of seizures. In this study, acute encephalopathy was defined as a condition characterized by decreased consciousness with or without other neurological findings, such as delirious behavior and seizures, lasting for 24 h or longer in children with infectious symptoms including fever, cough and diarrhea. The Annual Zao Conference mailing list includes more than 700 pediatric neurologists throughout Japan. From January 2012 to November 2013, we asked for enrollment of patients through the mailing list. A structured research form was given to the members of the mailing list to fill out if they had patients meeting the criteria. The completed research forms were returned to the first author by email. This study was approved by the Institutional Review Board of Juntendo University Faculty of Medicine. The patient data were collected anonymously.

The following items were included in the research form: age, gender, subtypes of acute encephalopathy, preexisting medical condition, prodromal illness and its pathogen, onset of acute encephalopathy, EEG monitoring, type of seizure (status epilepticus or clustering seizures), treatment for acute encephalopathy (steroids, intravenous gamma globulin, hypothermia), outcome, efficacy and adverse events of fPHT. We also asked the participants to describe the scheme of seizure time course and the use of antiepileptic drugs. In this study, AESD was defined as acute encephalopathy presenting with onset of prolonged seizures or status epilepticus, biphasic clinical course characterized by late worsening of consciousness along with clustering seizures or status epilepticus and widespread reduced diffusion in the cortex and/or subcortical white matter involving unilateral or bilateral hemispheres [1]. Any encephalopathy that did not meet the definition of AESD was classified into other encephalopathies. The efficacy of fPHT was categorized as follows based on clinical observation: effective; cessation of seizures, partially effective; 50% or more reduction in frequency and/or duration of seizures, ineffective; incompatible with the former two conditions.

Statistical analysis of the efficacy rate between the two groups was performed by Fisher's exact probability test for qualitative variables using the SPSS Statistics version 17.0 software (SPSS Inc., Tokyo, Japan). Statistical significance was accepted at a level of $p < 0.05$.

3. Results

The data of 38 children were obtained from 16 hospitals. fPHT was administered for 48 clinical events.

3.1. Demographic data

Demographic data are shown in Table 1. The age at onset of acute encephalopathy ranged from 16 days to 163 months (median, 27 months). There were 22 males (58%) and 16 females (42%). Eighteen children were categorized into the AESD group and 20 into the other encephalopathies group. Among subjects with other encephalopathies, two children were diagnosed as

Table 1
Demographic data of the patients.

	Total $n = 38$	AESD $n = 18$	Other encephalopathies $n = 20$
Age at onset (months)	27 (0.5–163)	22.5 (9–163)	23 (0.5–97)
Sex (M:F)	22: 16	13: 5	9: 11
Preexisting medical conditions			
None	37	17	20
Cerebral palsy	1	1	0
Prodromal illness			
Upper respiratory infection	16	8	8
Exanthema subitum	9	7	2
Gastroenteritis	5	0	5 (Rota in 4 and Noro in 1)
Influenza	3	1	2
Mycoplasma pneumonia	2	1	1
RSV bronchiolitis	1	0	1
Bacteremia	1	1 (*Moraxella catarrhalis*)	0
Herpes simplex encephalitis	1	0	1
EEG monitoring			
Intermittent EEG	16	10	6
Continuous EEG	5	2	3
Continuous aEEG	2	1	1
None	15	5	10
Treatment for acute encephalopathy			
Methylprednisolone pulse	31	16	15
Intravenous immunoglobulin	10	5	5
Hypothermia	4	1	3

The numerical variables were shown as median (range).
AESD: acute encephalopathy with biphasic seizures and late reduced diffusion, RSV: respiratory syncytial virus, aEEG: amplitude-integrated EEG.

having mild encephalopathy with reversible splenial lesion [6], one as ADEM, one as ANE and one as herpes simplex encephalitis. No specific diagnosis of acute encephalopathy was made in the other 15 children. The most common prodromal illness was non-specific upper respiratory infection, followed by exanthema subitum. EEG monitoring during the treatment with fPHT was performed in 23 children. However, continuous standard EEG or amplitude-integrated EEG (aEEG) was performed in only seven patients. Methylprednisolone pulse therapy was the most common treatment for the acute encephalopathy.

fPHT was used for 48 clinical events (Table 2) and was administered in two events during a single course of acute encephalopathy in eight children with AESD and two with other encephalopathies. Types of seizures were status epilepticus in 17 events and clustering seizures in 31. Before fPHT administration, no drugs were used in 18 events and one drug in 18. Two or more antiepileptic drugs were used in 12 events before fPHT administration and midazolam was the most frequently used, followed by diazepam.

Table 2
Background information at fPHT administration.

	Total $n = 48$	AESD $n = 26$	Other encephalopathies $n = 22$
Types of seizures			
Status epilepticus	17	9	8
Cluster	31	17	14
Number of AEDs before fPHT			
None	18	11	7
1	18	8	10
2	11	6	5
3	1	1	0
AEDs used before fPHT			
Midazoram	20	13	7
Diazepam	16	7	9
Thiopental	4	2	2
Phenobarbital	3	1	2

AED: antiepileptic drugs, fPHT: fosphenytoin.

3.2. Efficacy of fPHT

The median loading dose of fPHT was 22.5 mg/kg (range, 15–28 mg/kg). The median rate of injection was 2.8 mg/kg/min (range, 0.05–3.6 mg/kg/min). Serum PHT level was measured in 18 patients. The median serum PHT concentration was 10.55 μg/mL (range, 0.6–13.5 μg/mL) at 6–24 h after the initial administration.

Among a total of 48 clinical events, fPHT was effective in 34 (71%). Other antiepileptic drugs were used and failed to control seizures in 30 clinical events. Even

Table 3
Efficacy of fPHT.

	Total $n = 48$	AESD $n = 26$	Other encephalopathies $n = 22$
Status epilepticus			
Effective	11	6	5
Partially effective	2	0	2
Ineffective	4	3	1
Clustering seizures			
Effective	23	13	10
Partially effective	4	2	2
Ineffective	4	2	2

AESD: acute encephalopathy with biphasic seizures and late reduced diffusion.

in such situations, fPHT was effective in 21 events (70%). fPHT was effective in 19 of 26 (73%) clinical events in children with AESD and 15 of 22 (68%) events in children with other encephalopathies. The rate of events in which fPHT was effective did not differ between AESD and other encephalopathies. Regarding the type of seizures, fPHT was effective in 11 of 17 (65%) events with status epilepticus and 23 of 31 (74%) events with clustering seizures (Table 3). The rate of events in which fPHT was effective did not differ according to the type of seizure.

3.3. Adverse effects of fPHT

Arrhythmia, hypotension, obvious reduction of consciousness, local irritation, phlebitis and purple grove syndrome were not observed in any patient. One patient with apnea and oral dyskinesia had an unusually elevated serum PHT level (27.8 μg/mL) after a loading dose of 22.5 mg/kg followed by three maintenance doses of 7.5 mg/kg (84 h after the initial administration). fPHT was administered *via* peripheral venous line in 46 events and central venous line in 2. Extracellular fluid or maintenance solution was used and intravenous fluid incompatibility was not observed in any patient.

4. Discussion

In this study we showed that fPHT was effective and well tolerated when used for seizures in children with acute encephalopathy. fPHT efficacy did not differ according to subtype of acute encephalopathy or type of seizure. The rate of adverse effects was very low.

Complete cessation of seizures was achieved in 71% of children with acute encephalopathy. PHT efficacy was similar even after other antiepileptic drugs failed to control seizures. However, determining if fPHT is superior to other antiepileptic drugs is difficult. Presently, reports on the efficacy of other epileptic drugs for the treatment of seizures in children with acute encephalopathy are unavailable. The clinical effectiveness of fPHT in children with status epilepticus also remains unclear. Because fPHT is completely metabolized to PHT by phosphatases of the liver, red blood cells and many other tissues [7], its efficacy is comparable to that of PHT. Studies on the efficacy of PHT for the treatment of status epilepticus are limited [3]. In a randomized study of adults with status epilepticus, PHT was used as a first-line treatment in the early phase of status epilepticus with a success rate of 43.6%, which was inferior to treatment with lorazepam (64.9%) [8]. Agarwal et al. reported an 88% efficacy rate of PHT after diazepam failure in children and adults with status epilepticus, which was similar to intravenous valproate [9]. Comparative studies are necessary to determine the efficacy of individual antiepileptic drugs.

Complete cessation of seizures was obtained in approximately two-thirds of clinical events in children with AESD. Late seizures that appear along with deterioration of consciousness and MRI abnormalities are an outstanding feature of AESD and are often refractory to benzodiazepines. Excitotoxicity is considered to be closely related to the pathogenesis of AESD and seizure control is presumed important for avoidance of secondary brain damage [10,11]. In addition, AESD is a common subtype of acute encephalopathy in Japan and a majority of affected children have neurological sequelae, such as intellectual disability and attention deficit hyperactivity disorder [1]. While the superiority of fPHT to other antiepileptic drugs is presently uncertain, as mentioned above, we suggest that fPHT can be a drug of choice in cases of status epilepticus or clustering seizures in children with AESD, due to its high efficacy rate.

An important advantage of fPHT is its lack of sedative effect [3]. During the management of acute encephalopathy, evaluation of consciousness is important, especially in children. Excessive sedation was not observed in any patient, whereas sedative effects were evident after intravenous administration of benzodiazepines and phenobarbital. For this reason, fPHT may be superior to these drugs in children with acute encephalopathy.

Adverse effects of fPHT were infrequent in our study. fPHT is easier to administer than PHT because of its water solubility and neutral pH value [12,13]. A neutral pH level results in less common occurrence of serious reactions at the injection site, such as purple glove syndrome and skin necrosis. In our study, none of the children experienced complications at the injection site. The water solubility of fPHT contributes to lessening of the occurrence of intravenous fluid incompatibilities; indeed, route obstruction was not reported in this study. One of our patients with apnea and oral dyskinesia had a higher serum PHT level than the other patients. Several studies have suggested that maintaining the serum PHT concentration may be difficult in children because of their rapid elimination and cytochrome P450 enzyme induction [14]. Therefore, the patient with apnea and

oral dyskinesia might have metabolized fPHT poorly. Therapeutic serum level monitoring is necessary to reduce adverse effects of fPHT. Additionally, cardiovascular adverse effects—such as hypotension and arrhythmia—are the most serious complications of fPHT. Cardiovascular adverse effects were not observed in our patients, probably because the rate of infusion was usually monitored by the attending physicians. Continuous monitoring of electrocardiogram and blood pressure should be performed and the injection should be performed slowly when administering fPHT.

This study had several limitations. First, the data on efficacy and adverse effects may be inaccurate due to the retrospective design of the study. Prospective studies are necessary to determine the efficacy and safety of fPHT. The efficacy and safety of fPHT and other antiepileptic drugs were not compared. Whether fPHT is appropriate for patients with acute encephalopathy remains uncertain due to the lack of previous data on PHT. The results of this study suggested that fPHT is useful for patients with acute encephalopathy. Comparisons between fPHT and other epileptic drugs should be performed to determine the appropriate agent for use in patients with acute encephalopathy. The paucity of continuous EEG/aEEG monitoring is also problematic. Recent studies using continuous EEG monitoring have indicated the presence of nonconvulsive seizures in critically ill children or those with altered mental states [15,16]. Nonconvulsive seizures are difficult to recognize without EEG monitoring; thus, the efficacy of antiepileptic drugs should be determined on the basis of continuous EEG monitoring. Although aEEG is less sensitive, it can be useful for surrogate monitoring. Presently, continuous EEG/aEEG monitoring is not available in a majority of tertiary emergency hospitals in Japan; this must be overcome in the near future.

In summary, we showed that fPHT is effective and well tolerated among children with both AESD and other acute encephalopathies. Its efficacy did not differ according to the type of seizure and the presence or absence of prior antiepileptic treatment. fPHT can be useful for the treatment of seizures in children with acute encephalopathy. Further prospective studies comparing fPHT and other antiepileptic drugs should be performed to determine the appropriate treatment for children with acute encephalopathy.

Disclosure

We have read the Journal's position on issues involved in ethical publication and affirm that this report is consistent with those guidelines. None of the authors have any conflict of interest to disclose.

Acknowledgment

This work was partly supported by Grants from the Ministry of Health, Labor, and Welfare (H24-Shinkou-Ippan-002 and H22-Nanji-Ippan-028).

References

[1] Takanashi J, Oba H, Barkovich AJ, Tada H, Tanabe Y, Yamanouchi H, et al. Diffusion MRI abnormalities after prolonged febrile seizures with encephalopathy. Neurology 2006;66:1304–9.
[2] Mizuguchi M. Acute necrotizing encephalopathy of childhood: a novel form of acute encephalopathy prevalent in Japan and Taiwan. Brain Dev 1997;19:81–92.
[3] Trinka E. What is the relative value of the standard anticonvulsants: phenytoin and fosphenytoin, phenobarbital, valproate, and levetiracetam? Epilepsia 2009;50:40–3.
[4] Komatsu M, Okumura A, Matsui K, Kitamura T, Sato T, Shimizu T, et al. Clustered subclinical seizures in a patient with acute encephalopathy with biphasic seizures and late reduced diffusion. Brain Dev 2010;32:472–6.
[5] Hoshino A, Saitoh M, Oka A, Okumura A, Kubota M, Saito Y, et al. Epidemiology of acute encephalopathy in Japan, with emphasis on the association of viruses and syndromes. Brain Dev 2012;34:337–43.
[6] Tada H, Takanashi J, Barkovich AJ, Oba H, Maeda M, Tsukahara H, et al. Clinically mild encephalitis/encephalopathy with a reversible splenial lesion. Neurology 2004;63:1854–8.
[7] Fischer JH, Patel TV, Fischer PA. Fosphenytoin: clinical pharmacokinetics and comparative advantages in the acute treatment of seizures. Clin Pharmacokinet 2003;42:33–58.
[8] Treiman DM, Meyers PD, Walton NY, Collins JF, Colling C, Rowan AJ, et al. A comparison of four treatments for generalized convulsive status epilepticus. Veterans affairs status epilepticus cooperative study group. N Engl J Med 1998;339:792–8.
[9] Agarwal P, Kumar N, Chandra R, Gupta G, Antony AR, Garg N. Randomized study of intravenous valproate and phenytoin in status epilepticus. Seizure 2007;16:527–32.
[10] Mizuguchi M, Yamanouchi H, Ichiyama T, Shiomi M. Acute encephalopathy associated with influenza and other viral infections. Acta Neurol Scand 2007;115:45–56.
[11] Takanashi J, Tada H, Terada H, Barkovich AJ. Excitotoxicity in acute encephalopathy with biphasic seizures and late reduced diffusion. Am J Neuroradiol 2009;30:132–5.
[12] Eriksson K, Keränen T, Kälviäinen R. Fosphenytoin. Expert Opin Drug Metab Toxicol 2009;5:695–701.
[13] Bialer M. Pharmacodynamic and pharmacokinetic characteristics of intravenous drugs in status epilepticus. Epilepsia 2009;50:44–8.
[14] Takeoka M, Krishnamoorthy KS, Soman TB, Caviness Jr VS. Fosphenytoin in infants. J Child Neurol 1998;13:537–40.
[15] Abend NS, Sanchez SM, Berg RA, Dlugos DJ, Topjian AA. Treatment of electrographic seizures and status epilepticus in critically ill children: a single center experience. Seizure 2013;22:467–71.
[16] Greiner HM, Holland K, Leach JL, Horn PS, Hershey AD, Rose DF. Nonconvulsive status epilepticus: the encephalopathic pediatric patient. Pediatrics 2012;129:e748–55.

FULL-LENGTH ORIGINAL RESEARCH

Posterior quadrant disconnection surgery for Sturge-Weber syndrome

*Hidenori Sugano, *Hajime Nakanishi, *Madoka Nakajima, *Takuma Higo, *Yasushi Iimura, †Kyoko Tanaka, †Mariko Hosozawa, †Shinichi Niijima, and *Hajime Arai

Epilepsia, 55(5):683–689, 2014
doi: 10.1111/epi.12547

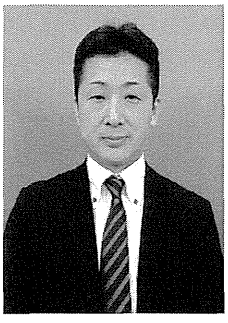

Hidenori Sugano is Assistant Professor and Director of Juntendo Epilepsy Center and a Neurosurgeon in the Department of Neurosurgery, Juntendo University, Tokyo, Japan.

Summary

Objective: Some patients with Sturge-Weber syndrome (SWS) need epilepsy surgery for adequate seizure control and prevention of psychomotor deterioration. The majority of patients with SWS have leptomeningeal angioma located over the temporal, parietal, and occipital lobes. We applied posterior quadrant disconnection surgery for this type of SWS with intractable seizure. We evaluated the efficacy of this procedure in seizure control and psychomotor development.

Methods: Ten patients who were surgically treated using the posterior quadrantectomy (PQT) were enrolled in this study. Surgical outcome was analyzed as seizure-free or not at 2 years after surgery. Psychomotor development was evaluated by the scores of mental developmental index (MDI) and psychomotor developmental index (PDI) in the Bayley Scales of Infant Development II preoperatively, and at 6 and 12 months after the PQT.

Results: Eight of 10 patients were seizure-free. Patients without complete elimination of the angiomatous areas had residual seizures. Average MDI and PDI scores before the surgery were 64.8 and 71.6, respectively. Scores of MDI at 6 and 12 months after the PQT in seizure-free patients were 80.5 and 84.5, respectively ($p < 0.01$). PDI scores at these postoperative intervals were 87.3 and 86.4, respectively ($p < 0.05$). Patients with residual seizures did not improve in either MDI or PDI.

Significance: The PQT achieved good seizure control and improved psychomotor development in patients with SWS. The complete deafferentation of angiomatous areas is required for seizure-free results and psychomotor developmental improvement.

KEY WORDS: Sturge-Weber syndrome, Epilepsy surgery, Posterior quadrantectomy, Seizure outcome, Psychomotor development.

Historically, intractable multilobar epilepsy has been treated with resective surgery, performing the removal of large parts of the hemisphere. However, superficial hemosiderosis occurs as a severe complication after large resective procedures.[1,2] Therefore, to prevent this complication, disconnection surgeries such as functional hemispherectomy and hemispheric differentiation, hemispherotomy, and posterior quadrantectomy were developed for these cases. Understanding that interruption of the epileptic discharge propagation pathways has the same effect as removing the focus, resection surgeries were effectively modified into disconnective ones.[3–8] Therefore, currently, disconnective surgeries yield the same or better results with lower complication rates compared to resections. This is valid also for the current approach to surgical technique in Sturge-Weber syndrome (SWS).

Recently, surgical treatment by multilobular resection or disconnection in cases of posterior quadrant located foci has been increasingly used, although the frequency of these procedures account for <5% of all epilepsy surgeries.[3] In the

Accepted January 4, 2014; Early View publication February 22, 2014.
Departments of *Neurosurgery and †Pediatrics, Juntendo University, Tokyo, Japan
Address correspondence to Hidenori Sugano, Department of Neurosurgery, Juntendo University, 2-1-1 Hongo, Bunkyo-ku, Tokyo 113-8421, Japan.
E-mail: debo@juntendo.ac.jp

majority of patients, the SWS leptomeningeal angioma involves the posterior quadrant, which justifies selective posterior quadrant disconnective surgery for this type of SWS. Similar to cases with intractable epilepsy due to complete unilateral hemispheric involvement, early surgery should be carried out for patients with epileptic foci in this area. In this study, we introduce the techniques and the details related to posterior quadrantectomy, and we evaluate its effectiveness for epilepsy control and psychomotor development.

Methods

We have followed 75 patients with SWS since 1986–2011 in Juntendo University, Tokyo, Japan. Clinical evaluation included clinical, electrophysiologic, neuroimaging, and neuropsychological examinations in all patients. The territory of leptomeningeal angioma was evaluated using magnetic resonance imaging (MRI) with contrast-enhanced fluid-attenuated inversion recovery (FLAIR) imaging.[9] We classified those patients into the following three groups according to the area involved by the leptomeningeal angioma: *bilateral*, *hemispheric*, and *partial*. We had six patients in the bilateral, 14 in the hemispheric, and 55 patients in the partial group. A hemispherotomy was indicated for all patients of the hemispheric group, and a corpus callosotomy was carried out for all of them in the bilateral group. Ten of 55 patients in the partial group were indicated for posterior quadrantectomy (PQT; Fig. 1).

We enrolled 10 patients with PQTs, six boys and four girls, in this study. The mean age at the time of surgery was 2 years and 4 months, and ranged from 8 months to 8 years. The postoperative follow-up period was from 24 to 47 months. In five patients the leptomeningeal angioma was in the left hemisphere, and in five it was in the right. Invasive EEG monitoring using subdural electrodes was indicated for one patient as a presurgical evaluation. That boy had continuous delay of psychomotor development; however, we did not confirm his clinical seizures on several occasions of video–scalp electroencephalography (EEG) monitoring. We speculated that he had several undetectable seizures that caused his developmental deterioration, and implanted subdural electrodes to confirm ictal activity. We obtained four subclinical seizures during 3 days of monitoring, and the seizure discharges came from within the posterior quadrant area. Postsurgical examinations were performed approximately every 6 months using clinical evaluation, assessment of seizure outcome, MRI, EEG, and neuropsychological batteries for all patients. We evaluated the seizure outcome, change of psychomotor development related to PQT in this study.

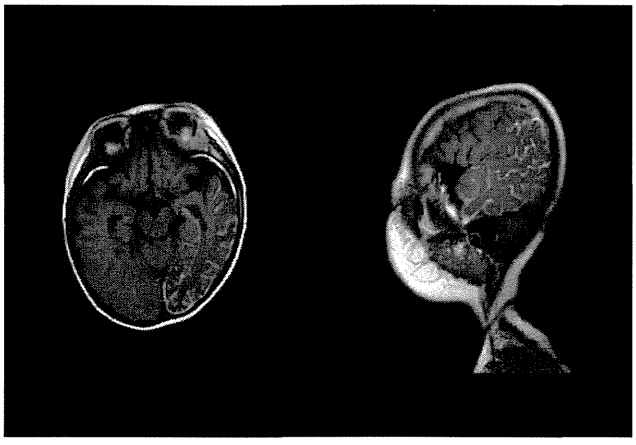

Figure 1.
Sturge-Weber syndrome with leptomeningeal angioma distributed in the posterior quadrant. The majority of our SWS patients (55/75) have the leptomeningeal angioma distributed in the temporal, parietal, and occipital lobes in our series. MRI with contrast-enhanced FLAIR imaging shows the accurate territory of leptomeningeal angioma. Ten of 55 patients were diagnosed with intractable epilepsy with continuous deterioration of psychomotor development and indicated for posterior quadrantectomy.

The posterior quadrantectomy surgical procedure

The patient's head was fixed on a horseshoe-shaped headrest 45 degrees rotation to the opposite side of the craniotomy. We used a neuronavigation system (Stealth station navigation system cranial application version 5; Medtronic, (Minneapolis, MN, U.S.A.) for this surgery. Before the skin incision, we simulated and decided on the disconnection line over the scalp using the neuronavigation system. Subsequently based on that we designed the craniotomy and the curvilinear scalp incision to expose adequate surgical field (Fig. 2).

After the craniotomy, we began with opening of the sylvian fissure. Because the temporal lobe is atrophic in almost all patients with SWS whose leptomeningeal angioma distributes in the posterior quadrant, the sylvian fissure is relatively easy to dissect. Widening the sylvian fissure provided adequate surgical field around the insular cortex and circular sulcus without brain retraction. The landmarks at this stage were the entire course of the circular sulcus, limen insulae, and M2 and M3 portions of the middle cerebral artery. Preservation of arteries and veins was preferable to reduce some not clearly predictable complications, such as postoperative temporal lobe swelling. The resection of cortex at the circular sulcus and white matter in the temporal stem was carried out and continued to the inferior horn of the lateral ventricle. Pes hippocampi and amygdala could be clearly observed at this stage. Subsequently, the amygdala was resected, and the uncinate fascicule was divided to disconnect anterior temporal lobe from frontal lobe. Disconnection of the temporal stem was continued to the posterior end of the circular sulcus, and the entire hippocampus from head to tail was exposed at this stage (Fig. 3).

Next, the direction of disconnection ascended to the parietal lobe. The line of disconnection of the parietal lobe was

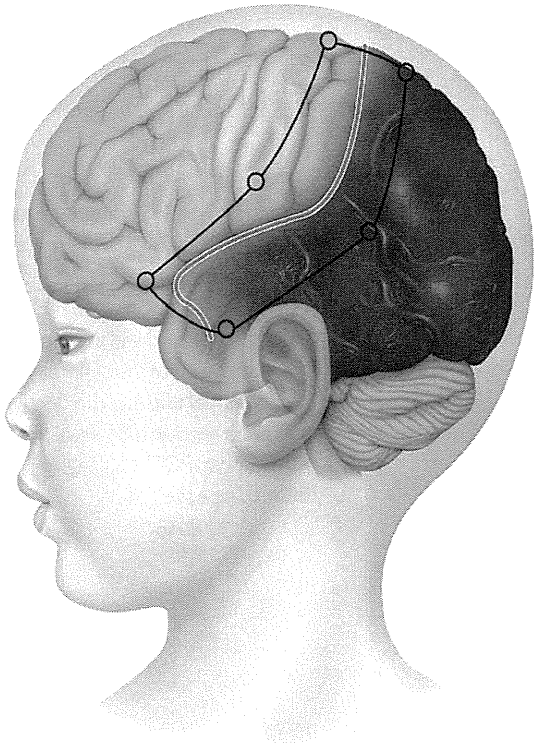

Figure 2.
Scalp incision. A curvilinear scalp incision is designed using the neuronavigation system as tracing over the supposed disconnection line. Craniotomy should be planned to obtain an adequate surgical field. Red line shows scalp incision, and black lines are margins of the free bone flap.

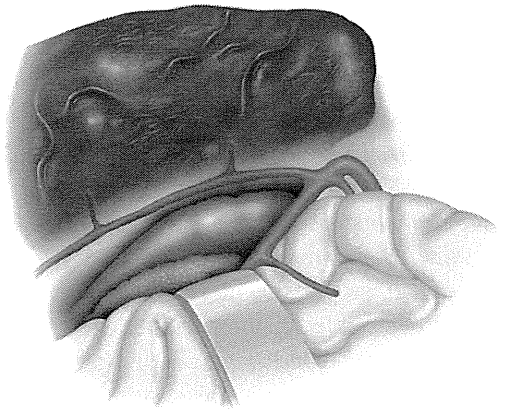

Figure 3.
Dissection of sylvian fissure. The key procedure of PQT is wide dissection of the sylvian fissure. Adequate surgical field can be obtained for exposure of limen insulae, circular sulcus, and branches of middle cerebral artery through the sylvian fissure. Temporal lobe disconnection can be accomplished from the circular sulcus to the inferior horn of lateral ventricle.

confirmed using neuronavigation. Central sulcus localization could be obtained by navigation and somatosensory evoked potentials. Disconnection at the distal end of circular sulcus was extended to operculum and convexity of the parietal lobe. Medial landmarks of this longitudinal disconnection were the choroid plexus and the falx. The splenium of corpus callosum was seen between the choroid plexus at trigonum and the falx. The commissural fibers through the splenium of corpus callosum should be divided at this stage. The vein of Galen and the velum interpositum under the divided splenium could be visualized through the arachnoid membrane just before completion of the posterior callosotomy. The distal fimbria was visible between the disconnected splenium and choroid plexus, and there they were divided to disconnect hippocampus. As a whole, the limbic network was deafferented by disconnecting fimbria and interfornicial commissure at this point, without hippocampectomy. Arachnoid membrane of the ambient cistern had to be completely exposed to guarantee the limbic disconnection. Surgical scheme and postsurgical MRI are presented in Figure 4.

The free bone flap was fixed back using absorbable plates. We did not insert any drainage tubes in ventricular, epidural, or subcutaneous spaces for this surgery.

Seizure and psychomotor developmental evaluation

Assessments of seizure outcome, clinical neurologic condition, MRI, and EEG were undertaken every 6 months after surgery. Seizure outcome was evaluated as seizure-free or residual seizures 24 month after the PQT. All patients continued the antiepileptic drugs after surgery at presurgical prescription and dosage for the same period.

The neuropsychological evaluations were performed using the Bayley Scales of Infant Development II (BSID-II) in Japanese translation.[10,11] These evaluations were done every 6 months after surgery for all patients younger than 4 years of age. One patient operated at the age of 8 was excluded in the neuropsychological evaluation using the BSID-II. We compared the preoperative results of mental developmental index (MDI) and psychomotor developmental index (PDI) in BSID-II to those 6 and 12 months after the PQT, respectively.

The BSID-II data were analyzed using SPSS version 18 for Windows (IBM SPSS, IBM Japan, Chuo-ku, Tokyo, Japan). Repeated measures analysis of variance (ANOVA) was performed to investigate the changes after the PQT on MDI and PDI, respectively. On analysis for MDI, because these data were satisfying for sphericity, we analyzed them using Mauchly's test of sphericity. On analysis for PDI, because these data were violating sphericity, we applied Greenhouse-Geisser test and Huynh-Feldt test. A p-value < 0.05 was considered statistically significant.

Results

Seizure and neurologic outcome

Eight of 10 patients resulted seizure-free after surgery. Two patients were initially seizure-free; however, their sei-

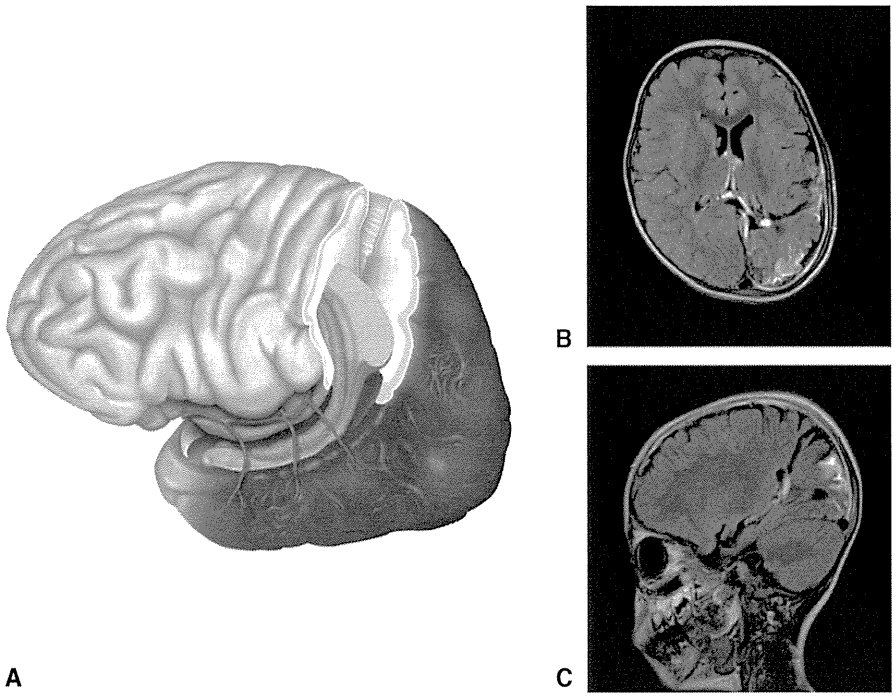

Figure 4.
Scheme of the PQT and postsurgical MRI. (**A**) The scheme presents the disconnection line of PQT. Pink zone represents the posterior callosotomy, and red area means disconnection of distal fimbria and hippocampal tail. See the detail in the Methods section. (**B**) Axial image of MRI in post-PQT. (**C**) Sagittal image of MRI in post-PQT.
Epilepsia © ILAE

zures recurred 3–6 months after surgery. Seizure recurrence in one of these patients had the same semiology and frequency as those of presurgery, whereas in the other they changed from dyscognitive to focal facial motor type. We concluded that an incomplete disconnection was done in the first case, and revised the PQT again at a second surgery. An uncompletely disconnected region was high in the parietal lobe convexity. This patient became seizure-free after the second surgery. For the second patient, we found other epileptic foci with the leptomeningeal angioma in the left insular cortex and frontal operculum that we had not found out at the initial neuroimaging evaluation. We added cortical resection for those regions at the second surgery, although his seizures continued even after that.

Seven of the 10 patients had leptomeningeal angioma within the posterior quadrant. Three patients had the angioma extending also to the frontal lobe. One patient had the leptomeningeal angioma in the insular and frontal operculum, and two patients had it in the motor cortex. A patient who had the leptomeningeal angioma in the insular and frontal operculum was already presented earlier. Two patients who had angioma in the motor cortex underwent additional cortical resections to the PQT. Those patients had postoperative hemiparesis. Their seizures were completely controlled but they needed rehabilitation, and finally their motor weakness recovered completely. We did not have any patients with speech disturbance after PQT, even after left posterior quadrant involvement. Hydrocephalus or superficial hemosiderosis were not observed in this series.

Psychomotor development

Impairment of the MDI and PDI in the BISD-II were observed in the patients with intractable seizures before surgery. Average MDI and PDI before surgery were 64.8 and 71.6, respectively. Average MDIs at 6 and 12 months after PQT were 80.5 and 84.5, respectively. Average PDIs at the same points of time were 87.3 and 86.4, respectively. We confirmed statistically significant improvements of MDI and PDI after PQT in patients who became seizure-free after surgery (Fig. 5). Dramatic catch up of psychomotor development appeared within the first 6 months and gradually continued after that. We had two cases with residual seizures, and they did not improve their developmental scores (Fig. 5).

Discussion

Our surgical indications for PQT in SWS were the following: well-localized leptomeningeal angioma in the posterior quadrant, confirmation of seizures originating from the same area from video–scalp EEG monitoring, and developmental delay. Sometimes, we experienced patients with SWS, who had progressive developmental deterioration without any detectable seizures or interictal epileptic discharges.[12,13] As we reported previously, progressive psychomotor deterioration could be a sole clue for having subclinical seizures in patients with SWS.[14] We considered indicated invasive EEG monitoring for patients with progressive developmental delay but undetectable clinical seizures in this study, and found several subclinical seizures. Relative findings leading to surgical decision are progressive atrophy and transient increase of glucose metabolism in the affected cerebral cortex on fluorodeoxyglucose–positron emission tomography (FDG-PET) study. Transient hypermetabolism within the affected area in SWS is known as a finding in recent seizures.[15–17] Therefore, we accept the transient hypermetabolism on FDG-PET study as a relative indication for epilepsy surgery. As a rule, surgical indica-

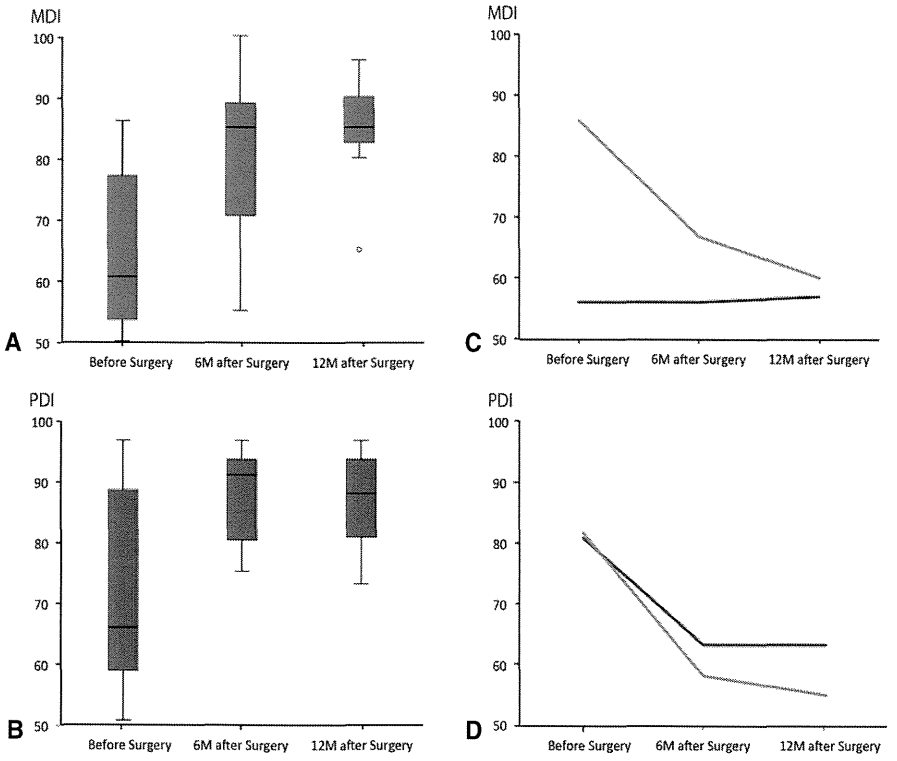

Figure 5.
Mental Developmental Index (MDI) and Psychomotor Developmental Index (PDI) in the Bayley Scales of Infant Development II (BSID-II). Average MDI and PDI before the surgery were 64.8 and 71.6, respectively. (**A**) MDIs at 6 and 12 months after the PQT in the seizure-free patients were 80.5 and 84.5, respectively ($p < 0.01$). (**B**) PDIs at those points were 87.3 and 86.4, respectively ($p < 0.05$). (**C, D**) Two patients with residual seizures continued deteriorating both in MDI and PDI even after the PQT.
Epilepsia © ILAE

tions should be decided from the findings of a comprehensive set of tests and examinations.

Our PQT procedure has much in common with the technique described by Daniel et al.,[3] but differs in the use of neuronavigation system, smaller craniotomy, and wide opening of the sylvian fissure. Our PQT is suitable for the case having temporal lobe atrophy. In cases with atrophy, it is easier to dissect the sylvian fissure and preserve vessels. The surgeon needs sufficient surgical field only around the sylvian fissure and the disconnection line of the parietal lobe. Short distance disconnection of the temporal stem from the circular sulcus exposing the inferior ventricular horn gives us certain surgical orientation. In SWS there are poorly developed sylvian veins and atrophic temporal lobe; therefore, SWS is anatomically appropriate for our modified PQT. The relatively limited surgical field in our modified PQT technique reduces surgical invasiveness and shortens surgical time. Our modified PQT can be used also for cases without atrophy; however, sylvian fissure dissection may require a larger technical effort because of the narrow space. The standard PQT might be a better choice in some of these cases.

Surgical outcome following multilobar surgery is generally accepted as worse than that of a single lobar resection.[18] Koszewski et al.[19] reported on a cohort of 93 patients with multilobar resection, and obtained Engel class I classification in 53% of them. In the series of Daniel et al.,[3] where they focused on surgery of the posterior quadrant, Engel class I outcome was 92% without any mortality or significant morbidity. They emphasized that completeness of removal or disconnection was essential for good surgical outcome. Although in some cases, such as cortical dysplasia, it is difficult to demarcate the margin of epileptic areas, the epileptic zone of SWS is almost equal to the distribution of the leptomeningeal angioma. Therefore, the surgeon should completely disconnect or remove cortex under the leptomeningeal angioma in SWS to obtain good surgical outcome.[20,21] In our series, patients in whom we could disconnect and/or remove the regions under the angioma became seizure-free. Hence, the most important factor for successful surgery in SWS is to delineate the margin of the leptomeningeal angioma on MRI. Postsurgical evaluation using MRI is mandatory to confirm the completeness of the surgery. We had two cases with residual seizures in this series and found that their angiomatous areas were not completely disconnected or eliminated. Since their seizures recurred within 6 months after surgery, we should accept the incompleteness of the initial surgical management within this period.

We had two patients whose leptomeningeal angioma distributed to the motor cortex, beyond the margins of the distinct posterior quadrant. Reorganization of motor function after epilepsy surgery has been already reported.[22,23] Functional recovery after motor cortex injuries was studied mainly in experimental models in animals, and functional imaging studies in humans.[24–28] The primary motor cortex in younger subjects is usually recovered better than the non-primary motor area in adults.[27] Areas that can compensate for motor function are reported in the premotor cortex, supplementary motor area, and parietal lobe in the affected hemisphere, and the contralateral hemisphere.[25,28–31] In order to compensate the motor function, only cortex

removal and not beyond, particularly not interfering with the descending corticospinal tract, is essential.[22,32] From these findings, resection of only the primary motor cortex with preserving underlining corticospinal tract in a young child can compensate motor function even after initial weakness. Therefore, in cases with a leptomeningeal angioma distributed in and beyond the posterior quadrant to the primary motor cortex, the surgeon should consider the PQT complemented with additional motor cortex removal to improve the surgical and developmental outcomes.

Speech function should be a concern, especially in dominant hemisphere surgery. Surgery before the age of 5 is favorable for speech recovery.[33,34] We did not have morbidity related to speech function. Except for an 8-year-old girl with left side involvement, all of our patients underwent surgery before the age of 4 years, and that might have been the reason for not having speech deficit. Speech function of our patients might have been readapted through neural plasticity after surgery, or even before that, as this is a congenital lesion. Although we could not evaluate the language mapping in the 8-year-old patient because she did not cooperate with the test, her speech function did not deteriorate after the PQT. Some reports support reorganization of speech areas even after the age of 8.[35,36] In children with progressively deteriorating psychomotor development due to intractable seizures, surgery aiming at psychomotor recovery has to be considered even in those older than 5 years. Lippe et al.[37] reported that brain plasticity after parietooccipital epilepsy surgery in young children allows for an acceptable scholastic level of cognitive skills such as reading and arithmetic. They also indicated that recovery of visual perceptive cognition is limited compared to verbal functions. Our patients after PQT have never complained about problems with their contralateral visual field areas, and their routine daily performance was as without having visual field defect. Pediatric patients after occipital or posterior quadrant resection or disconnection can compensate their visual field defect by unintentional moving of their eyes and/or head position. Because uncontrollable seizures are the reason for their deteriorated cognition, early epilepsy surgery for pediatric patients with posterior quadrant epileptic involvement offers the possibility of optimizing cognitive outcomes even at the expense of visual field defect.

Our PQT modification can achieve complete disconnection of the affected posterior quadrant through a small craniotomy and reduce the surgical invasiveness for patients with atrophic temporal lobe such as in SWS. The use of a neuronavigation system is required for surgical planning and is helpful for confirmation of complete disconnection during surgery, even with adequate understanding of interlobar connective anatomy. With seizure control as the main objective, the results of use of our PQT method showed it to be an effective technique to achieve it. Complete seizure control after surgery improved psychomotor development. Therefore, we can recommend this procedure for epileptic children with partial type of SWS involving mainly the posterior quadrant.

Acknowledgments

This work was partly supported by a Grant-in-Aid for Scientific Research (KAKENHI). Hidenori Sugano is funded by a Grant-in-Aid for Scientific Research (KAKENHI 24592173). Madoka Nakajima is funded by a Grant-in-Aid for Scientific Research (KAKENHI 23592106). Hajime Arai is funded by a Research Grant from the Ministry of Health, Labor and Welfare of Japan (2012-Nanchi).

Disclosure

None of the authors has any conflict of interest to disclose. We confirm that we have read the Journal's position on issues involved in ethical publication and affirm that this report is consistent with those guidelines.

References

1. Rasmussen T. Postoperative superficial hemosiderosis of the brain, its diagnosis, treatment and prevention. *Trans Am Neurol Assoc* 1973;98:133–137.
2. Villemure JG. Anatomical to functional hemispherectomy from Krynauw to Rasmussen. *Epilepsy Res Suppl* 1992;5:209–215.
3. Daniel RT, Meagher-Villemure K, Farmer JP, et al. Posterior quadrantic epilepsy surgery: technical variants, surgical anatomy, and case series. *Epilepsia* 2007;48:1429–1437.
4. Delalande O, Bulteau C, Dellatolas G, et al. Vertical parasagittal hemispherotomy: surgical procedures and clinical long-term outcomes in a population of 83 children. *Neurosurgery* 2007;60:ONS19–ONS32; discussion ONS.
5. Schramm J, Behrens E, Entzian W. Hemispherical deafferentation: an alternative to functional hemispherectomy. *Neurosurgery* 1995;36:509–515; discussion 15–6.
6. Schramm J, Kral T, Clusmann H. Transsylvian keyhole functional hemispherectomy. *Neurosurgery* 2001;49:891–900; discussion -1.
7. Shimizu H, Maehara T. Modification of peri-insular hemispherotomy and surgical results. *Neurosurgery* 2000;47:367–372; discussion 72–3.
8. Villemure JG, Mascott CR. Peri-insular hemispherotomy: surgical principles and anatomy. *Neurosurgery* 1995;37:975–981.
9. Griffiths PD, Coley SC, Romanowski CA, et al. Contrast-enhanced fluid-attenuated inversion recovery imaging for leptomeningeal disease in children. *AJNR Am J Neuroradiol* 2003;24:719–723.
10. Berk RA. The discriminative efficiency of the Bayley Scales of infant development. *J Abnorm Child Psychol* 1979;7:113–119.
11. Lung FW, Shu BC, Chiang TL, et al. Predictive validity of Bayley scale in language development of children at 6–36 months. *Pediatr Int* 2009;51:666–669.
12. Arzimanoglou A, Aicardi J. The epilepsy of Sturge-Weber syndrome: clinical features and treatment in 23 patients. *Acta Neurol Scand Suppl* 1992;140:18–22.
13. Jansen FE, van Huffelen AC, Witkamp T, et al. Diazepam-enhanced beta activity in Sturge Weber syndrome: its diagnostic significance in comparison with MRI. *Clin Neurophysiol* 2002;113:1025–1029.
14. Sugano H, Nakanishi H, Nakajima M, et al. Seizures continue even after prompt anti-epileptic drug medication in Sturge-Weber syndrome–study from prolonged video electrocoticography, a case report. *Childs Nerv Syst* 2009;25:143–146.
15. Alkonyi B, Chugani HT, Juhasz C. Transient focal cortical increase of interictal glucose metabolism in Sturge-Weber syndrome: implications for epileptogenesis. *Epilepsia* 2011;52:1265–1272.
16. Alkonyi B, Miao Y, Wu J, et al. A perfusion-metabolic mismatch in Sturge-Weber syndrome: a multimodality imaging study. *Brain Dev* 2012;34:553–562.
17. Chugani HT, Mazziotta JC, Phelps ME. Sturge-Weber syndrome: a study of cerebral glucose utilization with positron emission tomography. *J Pediatr* 1989;114:244–253.

18. Leiphart JW, Peacock WJ, Mathern GW. Lobar and multilobar resections for medically intractable pediatric epilepsy. *Pediatr Neurosurg* 2001;34:311–318.
19. Koszewski W, Czarkwiani L, Bidzinski J. Multilobar resections in surgical treatment of medically intractable epilepsy. *Neurol Neurochir Pol* 1998;32(Suppl. 2):81–94.
20. Arzimanoglou AA, Andermann F, Aicardi J, et al. Sturge-Weber syndrome: indications and results of surgery in 20 patients. *Neurology* 2000;55:1472–1479.
21. Bourgeois M, Crimmins DW, de Oliveira RS, et al. Surgical treatment of epilepsy in Sturge-Weber syndrome in children. *J Neurosurg* 2007;106:20–28.
22. Barba C, Montanaro D, Frijia F, et al. Focal cortical dysplasia type IIb in the rolandic cortex: functional reorganization after early surgery documented by passive task functional MRI. *Epilepsia* 2012;53:e141–e145.
23. Benifla M, Sala F Jr, Jane J, et al. Neurosurgical management of intractable rolandic epilepsy in children: role of resection in eloquent cortex. Clinical article. *J Neurosurg Pediatr* 2009;4:199–216.
24. Baciu M, Le Bas JF, Segebarth C, et al. Presurgical fMRI evaluation of cerebral reorganization and motor deficit in patients with tumors and vascular malformations. *Eur J Radiol* 2003;46:139–146.
25. Calautti C, Leroy F, Guincestre JY, et al. Dynamics of motor network overactivation after striatocapsular stroke: a longitudinal PET study using a fixed-performance paradigm. *Stroke* 2001;32:2534–2542.
26. Carey JR, Kimberley TJ, Lewis SM, et al. Analysis of fMRI and finger tracking training in subjects with chronic stroke. *Brain* 2002;125:773–788.
27. Rouiller EM, Olivier E. Functional recovery after lesions of the primary motor cortex. *Prog Brain Res* 2004;143:467–475.
28. Yoshiura T, Hasuo K, Mihara F, et al. Increased activity of the ipsilateral motor cortex during a hand motor task in patients with brain tumor and paresis. *AJNR Am J Neuroradiol* 1997;18:865–869.
29. Alkadhi H, Kollias SS, Crelier GR, et al. Plasticity of the human motor cortex in patients with arteriovenous malformations: a functional MR imaging study. *AJNR Am J Neuroradiol* 2000;21:1423–1433.
30. Cao Y, D'Olhaberriague L, Vikingstad EM, et al. Pilot study of functional MRI to assess cerebral activation of motor function after poststroke hemiparesis. *Stroke* 1998;29:112–122.
31. Chollet F, DiPiero V, Wise RJ, et al. The functional anatomy of motor recovery after stroke in humans: a study with positron emission tomography. *Ann Neurol* 1991;29:63–71.
32. Chamoun RB, Mikati MA, Comair YG. Functional recovery following resection of an epileptogenic focus in the motor hand area. *Epilepsy Behav* 2007;11:384–388.
33. Devlin AM, Cross JH, Harkness W, et al. Clinical outcomes of hemispherectomy for epilepsy in childhood and adolescence. *Brain* 2003;126:556–566.
34. Muller RA, Chugani HT, Muzik O, et al. Language and motor functions activate calcified hemisphere in patients with Sturge-Weber syndrome: a positron emission tomography study. *J Child Neurol* 1997;12:431–437.
35. Pataraia E, Billingsley-Marshall RL, Castillo EM, et al. Organization of receptive language-specific cortex before and after left temporal lobectomy. *Neurology* 2005;64:481–487.
36. Vargha-Khadem F, Carr LJ, Isaacs E, et al. Onset of speech after left hemispherectomy in a nine-year-old boy. *Brain* 1997;120 (Pt 1):159–182.
37. Lippe S, Bulteau C, Dorfmuller G, et al. Cognitive outcome of parietooccipital resection in children with epilepsy. *Epilepsia* 2010;51:2047–2057.

The contribution of epithelial-mesenchymal transition to renal fibrosis differs among kidney disease models

Tsutomu Inoue[1,2], Akihiro Umezawa[3], Tsuneo Takenaka[1], Hiromichi Suzuki[1,2] and Hirokazu Okada[1,2]

[1]*Department of Nephrology, Faculty of Medicine, Saitama Medical University, Saitama, Japan;* [2]*Division of Project Research, Research Center of Genomic Medicine, Saitama Medical University, Saitama, Japan and* [3]*Department of Reproductive Biology, National Institute for Child Health and Development, Tokyo, Japan*

The impact of the epithelial-mesenchymal transition (EMT) to the formation of renal fibrosis has been debated in several lineage-tracing studies, with conflicting findings. Such disparities may have arisen from varying experimental conditions such as different disease models, the mouse strain, and type of genetic alteration used. In order to determine the contribution of these factors to EMT, we generated four kidney disease models in several mouse strains genetically modified to express enhanced green fluorescence protein (EGFP) in cortical tubular epithelial cells under the control of the γ-glutamyl transpeptidase promoter. Using this approach, the EMT was visible and quantifiable based on a count of EGFP-positive interstitial cells in the fibrotic kidney sections of the four renal disease models found to be either EMT-prone or -resistant. The EMT-prone models consisted of unilateral ureteral obstruction and ischemic nephropathy in SJL mice. The EMT-resistant models consisted of ureteral obstruction in C57B/6 and F1 (C57B/6×SJL) mice, adriamycin nephrosis in 129 mice, and nephrotoxic serum nephritis in SJL mice. Analyses of these renal disease models suggest the emergence of EMT-derived fibroblasts arises in a disease-specific and strain-dependent manner. Thus, when considering molecular mechanisms and involvement of the EMT in renal fibrosis, it is important to take into account the experimental conditions, particularly the mouse strain and type of disease model.

Kidney International (2015) **87,** 233–238; doi:10.1038/ki.2014.235; published online 9 July 2014

KEYWORDS: interstitial fibrosis; obstructive nephropathy; renal tubular epithelial cells

Correspondence: *Hirokazu Okada, Department of Nephrology, Faculty of Medicine, Saitama Medical University, 38 Morohongo, Moroyama-machi, Iruma-gun, Saitama 350-0495, Japan.*
E-mail: hirookda@saitama-med.ac.jp

Received 15 August 2013; revised 17 May 2014; accepted 22 May 2014; published online 9 July 2014

The epithelial-mesenchymal transition (EMT) has been extensively studied in the context of embryonic development. The epithelia of mature tissues may also undergo EMT in response to stress, such as inflammation and wounding, leading to fibrogenesis.[1,2] The EMT is elicited under various conditions, including *in vitro* stimulation with transforming growth factor-β1, animal models of renal fibrosis,[3] and human obstructive nephropathy.[4] However, as the occurrence of EMT in experimental kidney disease models appears to be inconsistent, the contribution of EMT to the pathogenesis of renal fibrosis remains controversial.[5–7] We speculate that differences in experimental conditions, including the disease model, murine strain, and type of genetic modification used, may account for the discrepancies observed in the reports of EMT involvement in the setting of renal fibrosis. Here, we established an *in vivo* evaluation system for EMT, and examined differences in the contribution of EMT to renal fibrosis among several mouse models of renal disease. Strain-specific differences were also evaluated in the EMT-prone renal disease model.

RESULTS AND DISCUSSION

In a preliminary experiment, we recruited EMT-prone (MCT, mProx24, and NMuMG) and EMT-resistant (EpH4) cultured epithelial cells[8,9] and confirmed their responses to EMT-inducible stimulation with transforming growth factor-β1 and epidermal growth factor (EGF). In addition, cDNA microarray analyses were performed with RNA isolated from each cell line under conditions that promote EMT induction (GEO_ID No. GSE31359), and the top 10 upregulated EMT-specific genes were identified (Supplementary Table S1 online). Among these upregulated genes, the high-mobility group A2 (HMGA2) gene and Snail1 (both of which have been previously reported to be EMT-related transcription factors) were found to be significantly associated with the EMT in the MCT (Supplementary Figure S1 online). As is well known, the occurrence of the EMT in stimulated epithelial cells is not universal, even under controlled *in vitro* conditions. We therefore decided to assess both HMGA2 and Snail1 in the following *in vivo* experiments.

We subsequently established an *in vivo* evaluation system for the study of EMT based on a Cre recombinase/LoxP recombination system under the control of the γ-glutamyl-transferase (γ-GT) promoter in which kidney cortical tubular epithelial cells are permanently labeled with enhanced green fluorescent protein (EGFP). Using this system, we created γ-GT.Cre;EGFP double-transgenic (γGT-DTg) mice, which were then used to generate unilateral ureteral obstruction (UUO), ischemia–reperfusion injury, adriamycin toxicity (ADR), and nephrotoxic serum nephritis models. With the exception of the ADR model, we used fibrosis-prone SJL/J (SJL) mice[10] for all disease models, as the establishment of a progressive ADR model requires the 129S1/svImJ (129) background, which involves another type of fibrosis-prone mice.[10–12] In the normal kidneys of γGT-DTg mice, tubular epithelial cells appear green; however, no green interstitial cells were observed (Figure 1a). On the other hand, EGFP-positive interstitial cells were detected in the kidneys of the UUO and ischemia–reperfusion injury mice (Figures 1b and d, respectively), whereas only a few positive cells were found in the ADR and nephrotoxic serum nephritis mice (Figure 1e and f, respectively), indicating that the occurrence of EMT was influenced by the type of disease model. We stained the tissues for all models using Masson's trichrome staining and anti-fibronectin antibodies. It showed that interstitial fibrosis was evidently in progress in all models, regardless of the presence of EMT (Figure 2).

To verify the accuracy of our method for distinguishing interstitial cells from tubular epithelial cells, the tubular basement membranes were stained with periodic acid–Schiff (Figure 1c). Numerous green cells were observed not only in the intratubular regions but also in the intertubular regions representing the interstitium (Figure 1c). To determine the origin and properties of the EGFP-positive interstitial cells, the kidney samples obtained from the UUO mice were stained for heat-shock protein 47, CD45, and F4/80 cellular markers (Figure 3a–f). Almost all green interstitial cells were negative for CD45. The EGFP-positive cells were negative for F4/80. Numerous EGFP-positive cells were also heat-shock protein 47-positive, indicating that the population of interstitial cells was principally non-myeloidal/non-monocytic and also consisted of collagen-producing cells. We next evaluated the mRNA expression of HMGA2 and Snail1 using quantitative reverse transcriptase-polymerase chain reaction. In the UUO model, both EMT-related transcription factors were found to be significantly upregulated compared with those observed in the other models (Supplementary Figure S2 online).

Next, in order to examine the influence of the mouse genetic background, a UUO model was generated using γGT-DTg mice of strain C57BL/6J (B6), which have been well characterized as fibrosis-resistant strains,[10,12] and the first filial generation of strains B6 and SJL (F1). No GFP-positive cells were detected in the strain B6 or F1 γGT-DTg mice, although interstitial alterations were observed (Figure 1g and h, strain F1: B6×SJL). These findings are consistent with the results of previous studies in which the EMT was detected only at extremely low levels in the UUO, ischemia–reperfusion injury, and transforming growth factor-β1 transgenic mouse models of B6 mice or mixed genetic backgrounds that included B6 mice.[5–7] Therefore, the genetic background of the mice appears to be important for determining the susceptibility of the animals to EMT, as well as to renal fibrosis. We also previously reported that the F1 offspring of 129 and B6 mice display a phenotype similar to that of B6 mice.[10] Therefore, genes governing EMT susceptibility may also function in a recessive manner.

It is important to note that interstitial fibrosis progressed in the kidneys of both the ADR and nephrotoxic serum nephritis mice, even though few EMT events were detected. Although other lineage-tracing studies of the liver[13] and lungs,[14] as well as kidneys, of transgenic mice have confirmed the contribution of EMT to the development of organ fibrosis *in vivo*, our present results indicate that the EMT is not the only route for fibroblast development in adult fibrotic tissue. Fibroblasts are derived from residential stromal cells, including fibroblasts, endothelial cells,[15] and pericytes,[5,6] as well as infiltrating bone marrow–derived fibroblasts, such as fibroblast-specific protein-1-positive myeloid cells[1,16] and fibrocytes.[17,18]

In conclusion, our findings support the notion that, at least in the mouse kidney, the EMT promotes the development of interstitial fibrosis in both a disease-specific and strain-dependent manner. Although we were unable to identify the mechanisms underlying the differences in susceptibility to EMT, the difference in the expression levels of transcription factors, such as HMGA2 and Snail1, may provide us with a valuable clue to help clarify this issue. It is therefore important to consider the experimental conditions, particularly the mouse strain and disease model, when evaluating the involvement of EMT in the pathogenesis of renal fibrosis.

MATERIALS AND METHODS

Transgenic mice

Two types of transgenic mice, γ-GT.Cre and EGFP-reporter mice, were used in this study. γ-GT.Cre mice express Cre recombinase, primarily in the cortical tubular epithelia, under the control of γ-GT promoters.[1] EGFP-reporter mice carry an EGFP transgene with a floxed-STOP cassette for the fluorescence labeling of Cre-expressing cells.

In vivo experiments

Male 5- to 6-week-old double-transgenic line [γ-GT.Cre] x [floxed-STOP.EGFP] mice were used. Manipulations to generate each mouse renal disease model were carried out as previously reported.[11,14,19,20] The UUO, ischemia–reperfusion injury, nephrotoxic serum nephritis, and ADR mice models required 7, 14, 28, and 56 days, respectively, to develop appreciable numbers of interstitial cells. All animal experiments were conducted in accordance with the NIH Guidelines for the Care and Use of Laboratory Animals and approved by the Institutional Animal Care and Use Committee of Saitama Medical University. We histologically evaluated the progression of each disease model. As a result, the corresponding

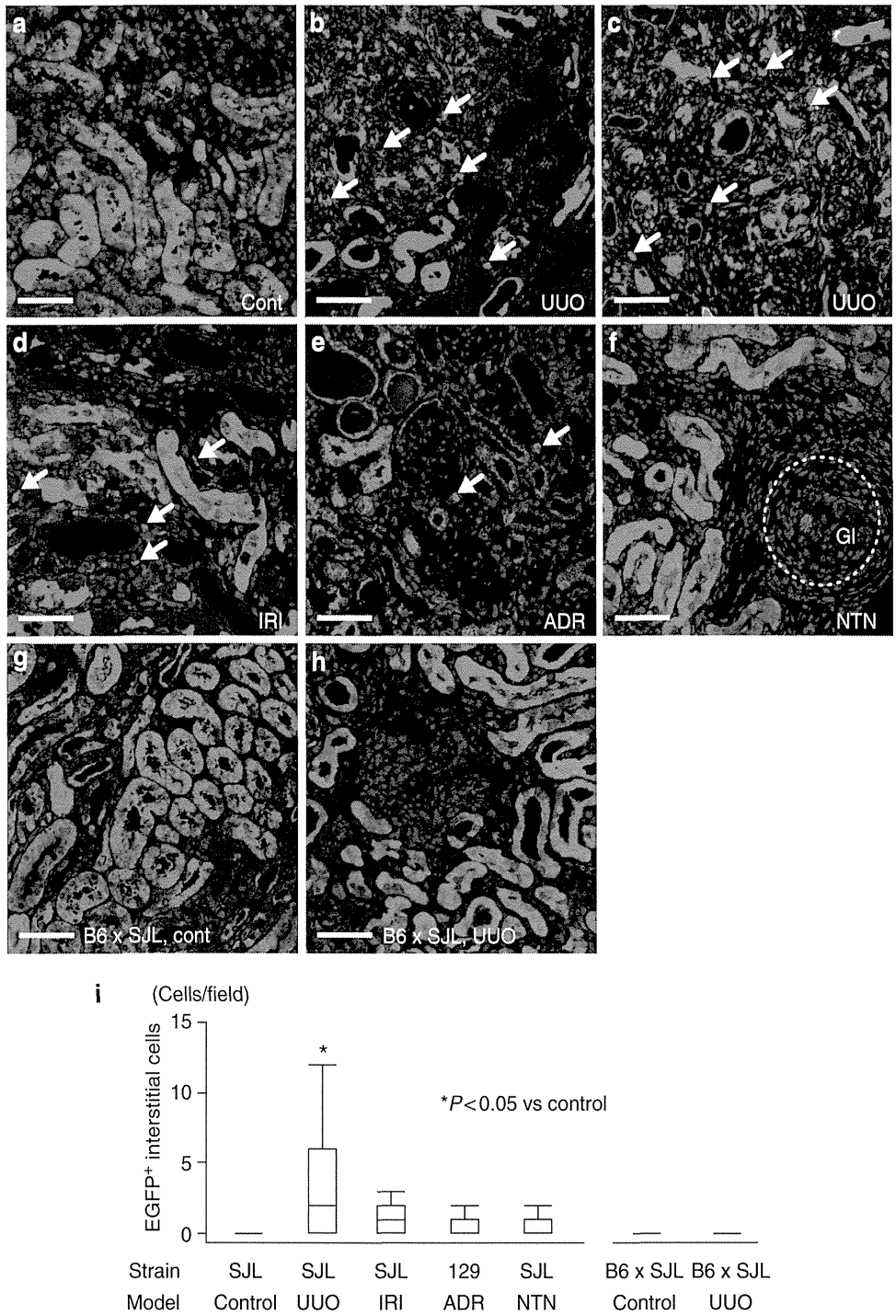

Figure 1 | Immunohistochemical analysis of the epithelial-mesenchymal transition (EMT) in the kidneys in various renal disease models established using γ-GT.Cre;EGFP double-transgenic mice. Cortical tubular epithelial cells expressing enhanced green fluorescence protein (EGFP) appear green and nuclei are stained blue. (**a**) In the control kidney, no interstitial green cells were observed. (**b**) In the kidneys of the unilateral ureteral obstruction (UUO) mice, green interstitial cells were found primarily in areas with severe tubulointerstitial alterations. (**c**) Periodic acid–Schiff (PAS) staining of the kidney sample in (**b**) showing the tubular basement membrane (red), which defines the border between the intratubular and intertubular regions (interstitium). Numerous green interstitial cells were also observed. (**d**, **e**, **f**): The ischemia–reperfusion injury (IRI) (**d**), adriamycin toxicity (ADR) (**e**), and nephrotoxic serum nephritis (NTN) (**f**) renal disease models exhibited different proportions of green interstitial cells among the total number of interstitial cells. Notably, few green interstitial cells were observed in the NTN model. (**g**, **h**) UUO model generated using γ-GT.Cre;EGFP double-transgenic mice with an F1(SJL×B6) mixed background. (**g**) In the control kidney, the majority of cortical tubular epithelial cells were stained green. (**h**) After the induction of the UUO model, few green interstitial cells were observed. (**i**) Enumeration of EGFP-expressing green interstitial cells. Significantly more green cells were detected in the kidneys of the UUO (SJL) mice than in those of the mice in the other renal disease models examined. The F1(B6×SJL) UUO mice had significantly fewer green cells than the SJL UUO model mice. The white arrows in all panels indicate EGFP-labeled interstitial cells that appeared to be derived from the tubular epithelium *via* EMT. Scale bar = 50 μm. The error bars indicate the standard deviation of five independent experiments. GI in (**f**) indicates the glomerulus.

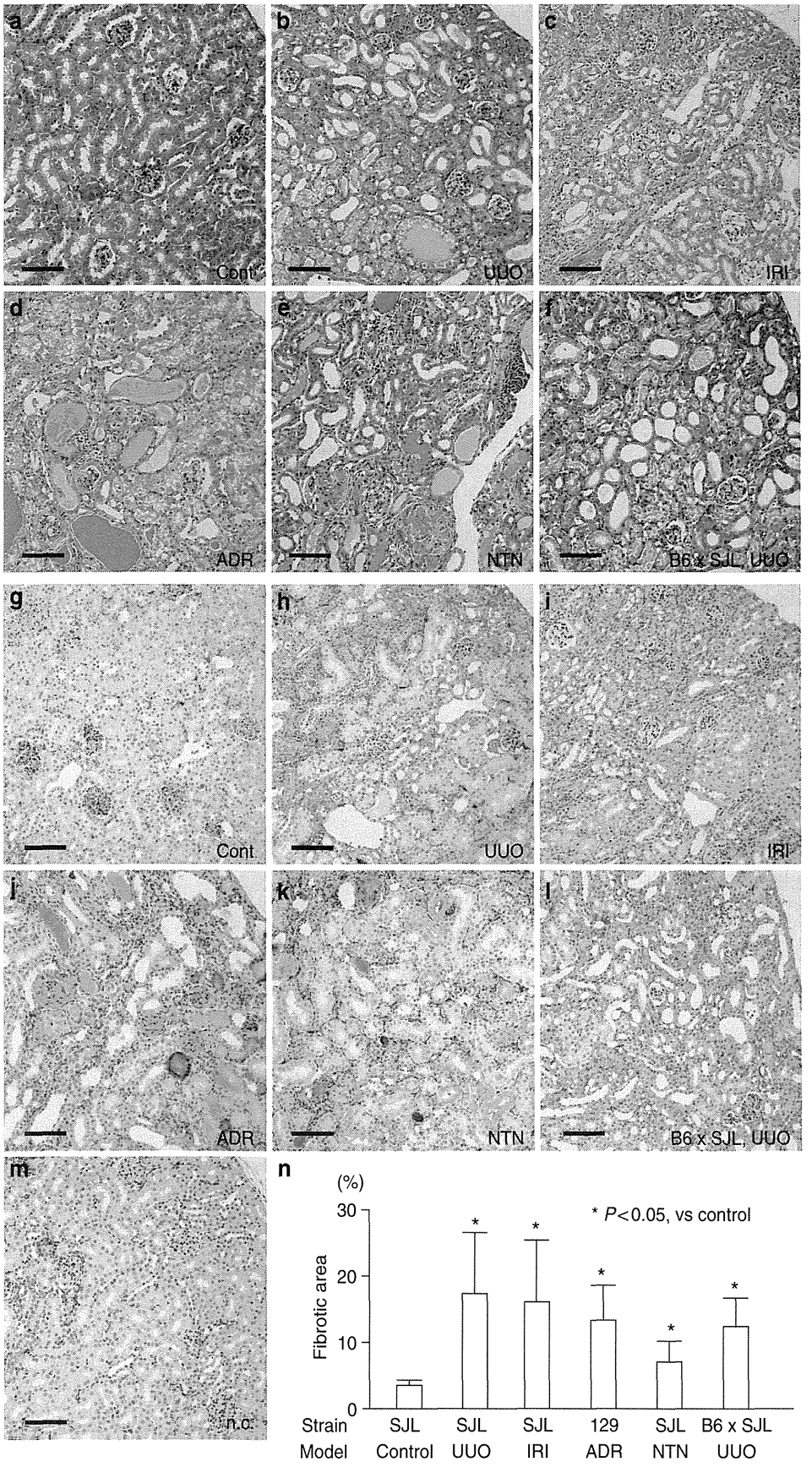

Figure 2 | Evaluation of interstitial fibrosis using Masson's trichrome staining and immunohistochemistry for fibronectin. Progression of collagen fiber deposition was observed in all disease models, regardless of the epithelial-mesenchymal transition (EMT)-prone or EMT-resistant status (**b**–**f**). In addition, fibronectin accumulation was noted in all models (**h**–**l**). Panels **a** and **g** are normal kidneys in SJL mice. Panel **m** indicates the findings of the negative control for immunohistochemistry using normal rabbit sera instead of anti-fibronectin antibodies. The results for the blue area of Masson's trichrome staining are shown in panel **n**. Scale bar = 200 μm (**a**–**m**). n.c. indicates negative control. The error bars indicate the standard deviation of five independent fields in each kidney obtained from the disease model and control groups (**n**).